

Methodology article

## A novel link between the proteasome pathway and the signal transduction pathway of the Bone Morphogenetic Proteins (BMPs)

Yin Lin<sup>4</sup>, Jennifer Martin<sup>1</sup>, Cornelia Gruendler<sup>1</sup>, Jennifer Farley<sup>1</sup>,  
Xianwang Meng<sup>1</sup>, Bi-Yu Li<sup>1</sup>, Robert Lechleider<sup>3</sup>, Carla Huff<sup>3</sup>,  
Richard H Kim<sup>3</sup>, William Grasser<sup>2</sup>, Vishwas Paralkar<sup>2</sup> and Tongwen Wang\*<sup>1</sup>

Address: <sup>1</sup>From Virginia Mason Research Center, 1201 Ninth Ave., Seattle WA 98101; Department of Immunology, University of Washington, Seattle, WA 98195; Department of Surgery/Genetics, Massachusetts General Hospital, Harvard Medical School, Boston, MA 02114, USA, <sup>2</sup>Dept. of Cardiovascular/Metabolic Diseases, Pfizer Inc., Eastern Point Rd., Groton, CT 06340, USA, <sup>3</sup>Laboratory of Chemoprevention, National Cancer Institute, 9000 Rockville Pike, 41/C629, Bethesda, Maryland 20892, USA and <sup>4</sup>Department of Molecular Genetics and Biochemistry, University of Pittsburgh, Medical school, PA15213, USA

E-mail: Yin Lin - yinlinn@yahoo.com; Jennifer Martin - jmartin@helix.mgh.harvard.edu; Cornelia Gruendler - weber@biomed.mat.ethz.ch; Jennifer Farley - jfarley@vmresearch.org; Xianwang Meng - x.meng@utoronto.ca; Bi-Yu Li - libiyu@yahoo.com; Robert Lechleider - rj124@georgetown.edu; Carla Huff - carlahuff@pol.net; Richard H Kim - RKim@genetics.com; William Grasser - william\_a\_Grasser@groton.pfizer.com; Vishwas Paralkar - vishwas\_m\_paralkar@groton.pfizer.com; Tongwen Wang\* - wangt@vmresearch.org

\*Corresponding author

Published: 21 June 2002

Received: 11 April 2002

*BMC Cell Biology* 2002, **3**:15

Accepted: 21 June 2002

This article is available from: <http://www.biomedcentral.com/1471-2121/3/15>

© 2002 Lin et al; licensee BioMed Central Ltd. Verbatim copying and redistribution of this article are permitted in any medium for any purpose, provided this notice is preserved along with the article's original URL.

### Abstract

**Background:** The intracellular signaling events of the Bone Morphogenetic Proteins (BMPs) involve the R-Smad family members Smad1, Smad5, Smad8 and the Co-Smad, Smad4. Smads are currently considered to be DNA-binding transcriptional modulators and shown to recruit the master transcriptional co-activator CBP/p300 for transcriptional activation. SNIP1 is a recently discovered novel repressor of CBP/p300. Currently, the detailed molecular mechanisms that allow R-Smads and Co-Smad to co-operatively modulate transcription events are not fully understood.

**Results:** Here we report a novel physical and functional link between Smad1 and the 26S proteasome that contributes to Smad1- and Smad4-mediated transcriptional regulation. Smad1 forms a complex with a proteasome  $\beta$  subunit HsN3 and the ornithine decarboxylase antizyme (Az). The interaction is enhanced upon BMP type I receptor activation and occur prior to the incorporation of HsN3 into the mature 20S proteasome. Furthermore, BMPs trigger the translocation of Smad1, HsN3 and Az into the nucleus, where the novel CBP/p300 repressor protein SNIP1 is further recruited to Smad1/HsN3/Az complex and degraded in a Smad1-, Smad4- and Az-dependent fashion. The degradation of the CBP/p300 repressor SNIP1 is likely an essential step for Smad1-, Smad4-mediated transcriptional activation, since increased SNIP1 expression inhibits BMP-induced gene responses.

**Conclusions:** Our studies thus add two additional important functional partners of Smad1 into the signaling web of BMPs and also suggest a novel mechanism for Smad1 and Smad4 to co-modulate transcription via regulating proteasomal degradation of CBP/p300 repressor SNIP1.

## Background

The bone morphogenetic proteins (BMPs) form a sub-family of the Transforming Growth Factor  $\beta$  (TGF- $\beta$ ) superfamily [1–4]. Members of the BMP family were initially identified by their ability to induce ectopic bone formation [4]. Functional characterization of BMPs and the cloning of new BMP family members have revealed that BMPs not only regulate bone formation and homeostasis but also function as morphogenetic factors for many other tissues and organs [2]. The critical regulatory roles of BMPs during early embryogenesis, such as neurogenesis, mesoderm formation and patterning, are also well-recognized [1–3].

Like other members of the TGF- $\beta$  superfamily, BMPs induce intracellular signaling via heteromeric complexes of the type I and type II serine-threonine kinase receptors [5,6]. The Smad family proteins are now known to function as key signal transducers downstream of the TGF- $\beta$  family type I receptors [6–8]. The activated BMP type I receptors directly recruit and phosphorylate a set of cytoplasmic Smad proteins that are specific for the BMP type I receptors. Three such BMP type I receptor-regulated Smads, Smad1, 5 and 8, have been identified [9]. Among them, Smad1 has been studied most extensively. The phosphorylation of Smad1 at the carboxylterminal SSVS motif triggers the release of Smad1 from the receptor, the formation of homo-oligomers of Smad1 and hetero-oligomers of Smad1 and Smad4, and the subsequent nuclear translocation of both Smad1 and Smad4 [6,9,10]. In the nucleus, Smad1 and Smad4 function as DNA-binding transcriptional regulators [9]. However, there is a unique feature in Smad-regulated transcription. Instead of independently binding to specific DNA sequence to regulate transcription, Smads are now considered to be transcriptional modulators since their ability to regulate transcription is dependent, in most cases, on their physical interaction with other nearby DNA-binding transcription factors [11]. Thus, one of the fundamental questions in understanding Smad-regulated transcription is how Smads function as transcription modulators.

The transcriptional regulatory activities of Smad1 in the nucleus are associated with its ability to directly bind to DNA [12], its interaction with other DNA-binding transcription factors, such as OAZ, SIP1 and Hoxc-8 [13–15], and also its interaction with the master transcriptional co-activator CBP/p300 [16]. Smad4 is an essential functional partner in Smad-regulated transcription and also interacts with CBP/p300 via a domain within the central linker region named as SAD (Smad Activation Domain) [13]. Since CBP/p300 has intrinsic histone acetyltransferase (HAT) activity and participates in chromatin remodeling, the recruitment of CBP/p300 into the DNA-binding complexes of Smad1 and Smad4 is likely a critical step in

Smad-regulated gene activation. However, our current knowledge of the molecular events involved in the recruitment of CBP/p300 and other transcriptional co-activators or co-repressors by Smads is still very limited. Furthermore, the molecular mechanisms underlying the cooperative functional partnership between Smad1 and Smad4 during transcriptional regulation is not yet understood.

Protein-protein interaction plays key roles in signal transduction. To gain further understanding of the signaling mechanisms of Smad1, we carried out a "blind" search for proteins that bind specifically to Smad1 using the yeast two-hybrid system. Characterization of these interactors reveals an unexpected physical and functional link between Smad1 and the proteasome-mediated degradation pathways. The 26S proteasome is responsible for the bulk turnover of cytoplasmic and nuclear proteins in eukaryotic cells and also plays a key role in the regulation of cell cycle, signal transduction, transcription as well as antigen presentation [17–21]. Most of the known proteasomal substrates are marked and targeted to proteasome by ubiquitination [17,19,20]. Ubiquitination, however, is not an obligatory step for substrate targeting to proteasome [17,18,20]. The degradation of the ornithine decarboxylase (ODC), the rate-limiting enzyme for polyamine synthesis, involves a protein named antizyme (Az), which binds and targets ODC to 26S proteasome for degradation [18]. However, ODC has remained an "orphan" in Az-dependent proteasomal degradation.

Interestingly, both ubiquitin and Az were isolated from the yeast two-hybrid system as Smad1 interactors. Furthermore, an integral component of proteasome, HsN3 [22–24], which is a  $\beta$  subunit of the 20S catalytic core, was also isolated as a strong and specific Smad1 interactor. Functional characterization of the interaction between Smad1, Az and HsN3 in the signaling pathways of BMPs led us to find a novel functional link between Smad1 and proteasome-mediated degradation events, through which a novel CBP/p300 repressor, SNIP1 [25], is removed to allow the transcriptional activation of BMP-responsive genes.

## Results

### ***The isolation of Smad1 interacting proteins reveals a physical interaction between Smad1 and components in proteasome-mediated degradation pathways***

We applied the yeast "Protein Trap" system to isolate Smad1 interactors [26,27]. Full length Smad1 was fused with the DNA-binding domain of LexA to serve as bait. A human fetal brain cDNA library with cDNA inserts fused with the transcriptional activation domain B42 was used for the screen. From screening one million cDNA clones, 40 clones exhibited strong activation of both of the reporter genes (LacZ and Leu2). Thirteen different cDNA inserts were identified from these 40 clones. The ability of

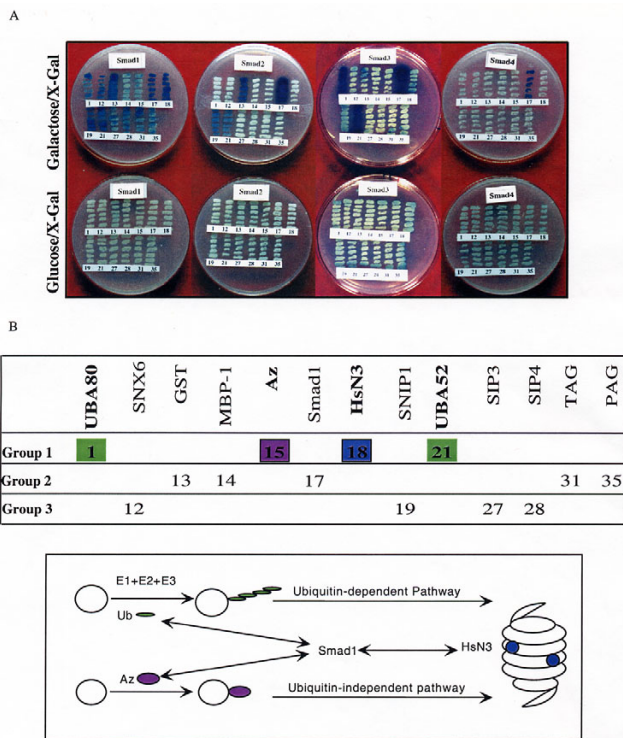


**Figure 1**  
**The isolation of Smad1 interacting proteins suggests a functional link between Smad1 and the 26S proteasome-mediated protein degradation.** **A.** Yeast two-hybrid test of the interaction specificity between thirteen isolated Smad1 interactors and Smad1, Smad2, Smad3 and Smad4. The "Protein Trap" system was used for the test [27]. Yeast EGY48 (*leu2, his3, trp1, ura3*) was first transformed with LexA fusion constructs of Smads in pEG202 vector and then transformed again with each of the thirteen different cDNA clones in pJG4-5 vector. The transformants were streaked onto selective plates of either galactose/raffinose (top) or glucose (bottom) lacking uracil, histidine and tryptophan (U-H-W) but containing X-Gal. The expression of the cDNA encoded fusion proteins is under the control of the GAL1 promoter. The light blue detected on the glucose plates reflects a basal level of transcriptional activation by the LexA-Smad fusion proteins. **B.** The thirteen Smad1 interactors were grouped into three groups based upon their known functions (top panel). The four clones that have functions along the proteasome-mediated degradation pathways are marked by different colors in the top panel and matches with the colored symbol in the bottom panel, which illustrates the proteasomal targeting pathways. See text for details.

these thirteen candidate Smad1 interactors to bind Smad1, Smad2, Smad3 and Smad4 were directly tested in the yeast two-hybrid system (Fig. 1A). Among the thirteen isolated Smad1 interactors, only clones 13, 17, 19 and 21 bind Smad2, whereas only clones 1, 17 and 21 exhibit strong interaction with Smad3. Only one clone (clone 17)

among the thirteen clones interacts with Smad4. Interestingly, this clone encodes a truncated Smad1 lacking its MH1 domain. Such an interaction is consistent with the known ability of Smad1 to bind Smad4 upon its activation in mammalian cells [9].

The identities of the thirteen interactors are summarized (Fig. 1B, top panel). We divided the interactors into three groups (Fig. 1B, top panel). The first group contains proteins that have a functional link to the degradation pathways of the 26S proteasome. They are: two ubiquitin precursors UBA80 (clone 1) and UBA52 (clone 21), the ornithine decarboxylase antizyme (Az) (clone 15) and the proteasome  $\beta$  subunit HsN3 (clone 18). The second group contains four known proteins: GST (clone 13), MBP-1 (c-Myc promoter Binding Protein, clone 14) [28], Smad1 (clone 17), TAG (Tumor Associated Gene, clone 31) [29] and PAG (Proliferation Associated Gene, clone 35) [30]. The third group contains four novel proteins: clone 19, 12, 27 and 28, which we named as SNIP1, SIP2, SIP3 and SIP4, respectively. The functional characterization of clone 19 (SNIP1) as a novel CBP/p300 interactor and repressor has been reported recently in the signaling pathways of TGF- $\beta$  [25]. The functional characterization of clone 12 (SIP2) as a new member of the sorting nexin family member has also been reported [31]. Studies of the novel protein SIP3 will be reported separately (Paralkar et al, manuscript in preparation).

We were intrigued by the fact that Smad1 binds to Ub, Az and HsN3, all of which are involved in proteasome-mediated degradation pathways, as illustrated in Fig. 1B, bottom panel. The well-known ubiquitin-dependent pathway involves the covalent attachment of ubiquitin to substrate proteins to form polyubiquitin chain, which then targets the marked substrates to proteasome for degradation [17,19,20]. The ubiquitin-independent pathway is not well defined, but involves targeting proteins other than ubiquitin. The best-characterized example of ubiquitin-independent degradation is the degradation of ornithine decarboxylase (ODC), which is dependent upon ODC interaction with the targeting protein antizyme (Az) [18]. How ubiquitinated substrates or Az-bound ODC is recognized by the 26S proteasome is not well understood. HsN3 is a  $\beta$  subunit of the 20S core of the 26S proteasome and previously has also been implicated in targeting its interacting protein p105 subunit of NF- $\kappa$ B into the 26S proteasome [22-24,32]. Thus, it is interesting that Smad1 can bind to two types of proteasome substrate-targeting proteins (ubiquitin and Az) as well as a proteasome component (HsN3) that has a possible substrate-targeting role. Studies were then carried out to further characterize Smad1 interaction with HsN3 and Az in mammalian cells and test a functional role of these interactions in the signaling pathways of BMPs as detailed below.

**Smad1 interacts with prosequence-containing HsN3 but not processed HsN3 in the 20S proteasome and the activation of the BMP type I receptor enhances the interaction**

We first focused upon the physical interaction between Smad1 and HsN3. As one of the seven  $\beta$  subunits of the 20S proteasome, the newly translated HsN3 has an N-terminal 44 amino-acid prosequence, which is processed upon the complete assembly of HsN3 into the mature 20S proteasome [22–24]. The assembly of the 20S proteasome involves multiple steps and the formation of assembly intermediates [33–36]. As illustrated in Fig. 2A, seven single  $\alpha$  subunits first form the  $\alpha$  ring, which serves as the template for seven  $\beta$  subunits to assemble the  $\beta$  ring. The half proteasomes containing one  $\alpha$  and one  $\beta$  rings are further assembled into 20S proteasome, a process involving the proteolytic cleavage of the prosequences of five  $\beta$  subunits, including HsN3. The 20S proteasome then combines with two 19S regulatory complex to form the 26S proteasome, which is the degradation machinery responsible for both ubiquitin-dependent and ubiquitin-independent degradation [37]. The prosequences of the proteolytic  $\beta$  subunits are important to keep the proteolytic sites inaccessible to the substrates. In addition, the prosequences still bind to the  $\beta$  subunits after its cleavage and may serve important chaperon roles for the  $\beta$  subunits to be properly positioned into assembly complex. This was demonstrated previously by artificially removing the prosequence of one  $\beta$  subunit and showed that the assembly of this  $\beta$  subunit is completely blocked while separate expression of the prosequence was enough to restore the assembly [19]. The defective assembly of a  $\beta$  subunit due to the lack of prosequence is illustrated in Fig. 2B.

To follow up the observed interaction between Smad1 and HsN3 in mammalian cells, we first constructed three HsN3 expression constructs. The first construct contains a Flag-epitope placed at the C-terminus of HsN3 (N3-F), since the C-terminus of HsN3 is not buried inside of the mature proteasome, according to the crystal structure of HsN3 [38]. The second and the third constructs contain either the Flag or the T7 epitopes placed at the N-terminus of HsN3 (F- $\Delta$ N3, T7- $\Delta$ N3). Since the N-terminal prosequence of HsN3 is processed upon assembly into the 20S proteasome, we deleted the prosequence of HsN3 and replaced it with the Flag/T7-epitopes to assure that the epitopes will not be lost due to prosequence-processing. We first expressed these constructs into COS1 cells and examined their expression and assembly properties by immunoprecipitation of each expressed protein from metabolically labeled COS1 cells (Fig. 2C). Multiple endogenous proteins from COS1 cells were co-precipitated with Flag tagged wild type HsN3 (Fig. 2C, lane 2), while much few proteins were detected in the immunoprecipitates of the two deletion versions of HsN3 lacking the prosequence (Fig. 2C, lanes 3 & 4). The predominant

band in the immunoprecipitation of wild type HsN3 is the prosequence-containing HsN3 (Pro-N3-F), as indicated by its molecular weight and the ability of anti-Flag antibody to detect it in a parallel Western blot. The other predominant band immediately below Pro-N3-F is the mature form of Pro-N3-F, as indicated by the ability of this band to be also detected by anti-Flag on the Western blot and by its co-migration with the deletion version of N3 lacking the prosequence (F- $\Delta$ N3 in lane 3). The rest of the proteins detected in the immunoprecipitates of wild type full length HsN3 (Fig. 2C, lane 2) are predominantly different subunits of the 20S proteasome and 19S regulators, as indicated by their molecular weights and their ability to be recognized by anti-20S and anti-19S antibodies (data not shown). The lack of most of these endogenous proteasome components in the immunoprecipitates of the two deletion version of HsN3 whose prosequences have been artificially removed via deletions indicates that the prosequence of HsN3 is also important for its successful assembly into the mature 20S proteasome. The slight different band patterns detected in the immunoprecipitates of F- $\Delta$ N3 and T7- $\Delta$ N3 suggests that different epitope tags may influence N3 interaction with endogenous proteasome components. Since mature  $\beta$  subunits are only found in the 20S proteasome [19], the detection of the mature form of the Flag-tagged HsN3 assured us that the exogenous Flag-tagged HsN3 proteins are normal in their ability to be incorporated into the 20S proteasome.

We then tested the ability of HsN3 to bind Smad1 in COS1 cells by transient transfection followed by immunoprecipitation assays. To monitor the co-precipitation of Smad1 with HsN3-containing proteasome complexes, immunoprecipitation were carried out using total cellular proteins from metabolically labeled COS1 cells. Upon the immunoprecipitation of Smad1, only the full-length HsN3 protein, but not the processed mature form of HsN3, was detected to co-precipitate with Smad1 (Fig. 3A, right panel, lane 4). Although the overexpressed HsN3 is associated with many other endogenous proteasome components from the COS cells (Fig. 3A, left panel, lane 4), these endogenous proteins also were not detected in the immunoprecipitates of Smad1 (Fig. 3A, right panel, lane 4). Thus, Smad1 only binds the prosequence-containing HsN3 (pro-N3-F), which, as illustrated in Fig. 2A, only exists transiently before the formation of 20S proteasome. Our domain mapping studies in yeast two-hybrid system have previously suggested that the MH2 domain of Smad1 is necessary for its interaction with HsN3 [39]. Thus we also tested the interaction between HsN3 and Smad1 MH2 domain. Pro-N3-F was also detected in the immunoprecipitates of Smad1MH2 (Fig. 3A, right panel, lane 3), suggesting that the MH2 domain is sufficient to bind to the pre-assembled HsN3.

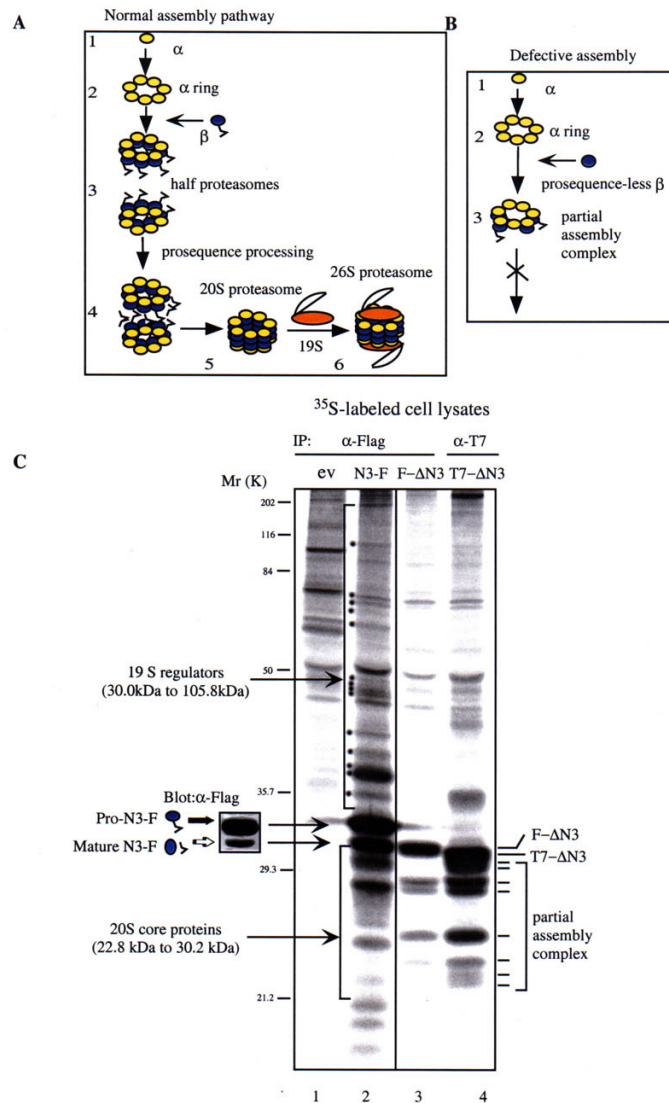


**Figure 2**  
**The expression and assembly of HsN3 in transfected COS1 cells.** **A.** A cartoon that illustrates the multiple steps known to involve in the assembly of the 26S proteasome. See text for details. **B.** A cartoon that illustrate the importance of  $\beta$  subunit prosequence in proteasome assembly. See text for details. **C.** The different assembly properties of wild type HsN3 and mutant HsN3 lacking its prosequence in transfected COS1 cells. COS1 was transfected with N3-F, a construct that contains the full-length wild type HsN3 and a Flag-epitope at the C-terminus (lane 2), or with F- $\Delta$ N3 (lane 3), a construct that lacks its prosequence at the N-terminus, instead contains an N-terminal Flag-epitope, or with T7- $\Delta$ N3, a construct that similarly lacks the prosequence but contains an N-terminal T7-epitope (lane 4). Cells were metabolically labeled with <sup>35</sup>S-methionine for 4 hrs before cells were harvested and analyzed by immunoprecipitation, as indicated. The two major bands in lane 2 were detected by Western blot using anti-Flag and marked out as prosequence-containing HsN3 (Pro-N3-F) and mature HsN3 (mature N3-F). The endogenous proteasome components at the molecular weight range of 19S proteasome (marked by small dots) or 20S proteasome in lane 2 are marked with brackets. A distinct set of eight bands that commonly detected to be associated with F- $\Delta$ N3 or T7- $\Delta$ N3 is marked with short lines at the right side of the panel. The transfection efficiency was monitored by co-transfection with a GFP construct. Equal transfection efficiency (70–80%) among different samples in a single experiment was the pre-requisite for metabolic labeling and the subsequent immunoprecipitation assays. Equal total amount of proteins were used for immunoprecipitation.

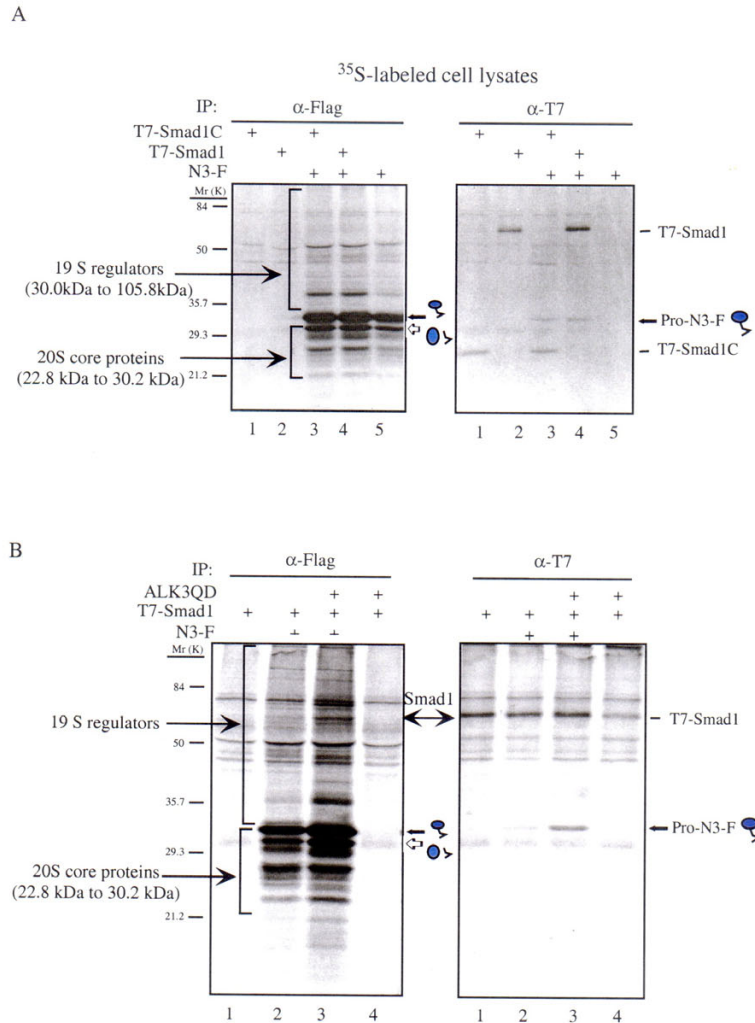


**Figure 3**  
**Smad1 interacts with the pre-assembled HsN3 and BMP type I receptor activation enhances the interaction.****A.** The prosequence-containing form (pre-assembled form) of HsN3 interacts with Smad1 or the MH2 domain of Smad1 (Smad1C) in COS cells upon co-expression. COS cells were transiently transfected with the indicated plasmids and metabolically labeled with <sup>35</sup>S-methionine for the last 4 hrs. Cell lysates were immunoprecipitated with either anti-Flag to detect HsN3 (left panel) or with anti-T7 to detect Smad1 and Smad1C (right panel). The co-precipitated prosequence-containing HsN3 in both panels is marked by a filled arrow and labeled as "Pro-N3-F" and a cartoon symbol shown in Fig. 2A. The mature HsN3 is marked by an open arrow and labeled by a cartoon symbol with the cleaved prosequence next to the mature HsN3. **B.** The activation of BMP type I receptor ALK3 enhances the interaction between Smad1 and the pre-assembled HsN3. Methods are same as in Fig. 2C.

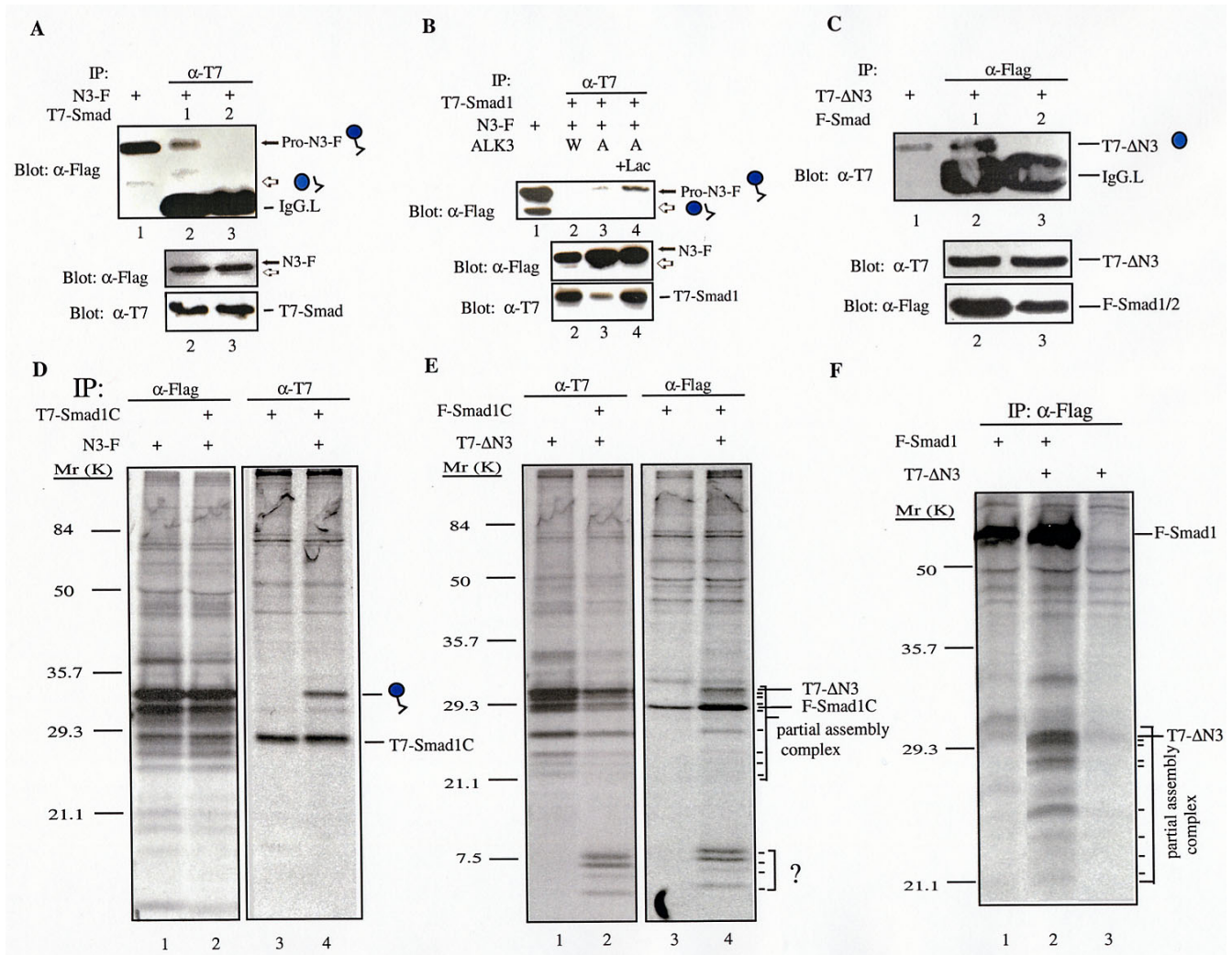


**Figure 4**  
**Western blot analyses to confirm Smad1 interaction with prosequence-containing HsN3 and the detection of Smad1 interaction with HsN3 assembly intermediates.** **A&B.** Immunoprecipitation and Western blot analyses of specific interaction between Smad1 and the prosequence-containing HsN3. COS1 cells were transfected with the indicated full length HsN3 and Smad1 or Smad2 and the interaction was analyzed via immunoprecipitation followed by Western blot, as indicated. Lactacystin treatment (indicated in panel **B.**, lane 4) was 8 hrs. The co-precipitated prosequence-containing HsN3 and the naturally processed mature HsN3 is marked and labeled similarly as in Fig. 3. "Ig.G.L" represents antibody light chain. **C.** The interaction between Smad1 and prosequence-containing HsN3 is not dependent upon the prosequence of HsN3. T7-ΔN3: T7-tagged deletion mutant of HsN3 that lacks the prosequence. To distinguish this form of mutant HsN3 from the naturally processed HsN3 in panels **A** & **B**, T7-ΔN3 is also labeled with a cartoon symbol that matches the assembly defective β subunit shown in Fig. 2B. **D.-F.** Smad1 and Smad1C (MH2 domain) both bind to HsN3-associated proteasome assembly intermediates accumulated as a result of artificial removal of the prosequence of HsN3. COS1 cells were transiently transfected with the indicated constructs, labeled with <sup>35</sup>S-methionine for 4 hrs before cells were harvested and analyzed by immunoprecipitation, as indicated. The eight distinct bands associated with T7-ΔN3 as shown in Fig. 2C is again marked here in lanes 2 and 4 in panel **E**. An additional four distinct small molecular weight bands are also detected in these two lanes, as marked by "?". The identities of these proteins are unknown, but they were always detected only when Smad1C and ΔN3 were co-expressed.

To test whether the observed interaction between Smad1 and Pro-N3-F, the pre-assembled form of HsN3, is regulated by BMP type I receptor activation, we co-expressed Smad1 and HsN3 with a mutant type I receptor,

ALK3Q233D. ALK3Q233D is constitutively active in inducing downstream signaling events in the absence of BMPs or the type II receptor [40]. The co-expression of ALK3Q233D with Smad1 and HsN3 significantly in-

creased the amount of the pre-assembled HsN3 that was co-precipitated with Smad1 (Fig. 3B, right panel, compare lanes 2 & 3). Smad1 was also detected in the immunoprecipitates of HsN3 (Fig. 3B, lanes 2 & 3). Since equal transfection efficiency was monitored and equal total proteins were used for the immunoprecipitation, the increased signals of pro-N3-F and its associated proteins in Fig. 3B, lane 3, left panel, may reflect an increased stability of HsN3 due to complex formation with Smad1, upon BMP receptor activation.

The association between Smad1 and HsN3 was further confirmed by immunoprecipitation followed by Western blot analyses. As shown in Fig. 4A and Fig. 4B, Pro-N3-F was specifically detected in the immunoprecipitates of Smad1 but not those of Smad2. When the activated BMP type I receptor was co-expressed with Smad1 and HsN3, a reduction of Smad1 level was detected and the reduction is blocked by the addition of the proteasome inhibitor lactacystin, indicating the proteasomal degradation of Smad1 induced by BMP type I receptor activation. This phenomenon was further investigated and confirmed in a separate study [39]. The interaction between Pro-N3-F and Smad1 was also stabilized in the presence of proteasome inhibitor lactacystin (Fig. 4B, lanes 4). Western blot using anti-26S proteasome was also carried out to show that only Pro-N3-F, not mature N3, nor other proteasome components, was co-precipitated with Smad1 (data not shown).

#### **Smad1 can interact with prosequence-deleted HsN3 in HsN3 assembly intermediates**

The lack of mature HsN3 and other proteasome components in the immunoprecipitates of Smad1 could be mediated by two different mechanisms. First, the prosequence of HsN3, which is processed from the mature HsN3, is necessary for Smad1 to bind to HsN3. Second, the final maturation of the 20S proteasome resulted from the assembly of two half proteasomes into the four stacked ring structure could trap the already bound Smad1 inside the proteasome for rapid degradation or lead to the dissociation of Smad1 from mature 20S proteasome due to the inaccessibility of Smad1 binding site on the incorporated HsN3. We first tested the role of the prosequence of HsN3 in binding to Smad1. As shown in Fig. 4C, artificial removal of the prosequence of HsN3 ( $\Delta$ N3) did not abolish Smad1 binding to HsN3. In fact, the interaction between  $\Delta$ N3 and Smad1 was even stronger when directly compared with the interaction between wild type HsN3 and Smad1 (data not shown). Thus, HsN3 does not require the prosequence to bind Smad1. Since we have shown that artificial removal of the prosequence of HsN3 leads to a blockage of the normal assembly of HsN3 into the mature proteasome (Fig. 2C), we suspect that the detected strong signals of  $\Delta$ N3 from

Smad1 immunoprecipitates reflect the accumulated HsN3 within the defective assembly intermediates, as illustrated in Fig. 2B. To test this possibility, we directly compared the ability of Smad1 MH2 domain to bind wild type HsN3 and prosequence-less mutant HsN3 in metabolically labeled COS 1 cells (Fig. 4D & 4E). When COS1 cells were expressing wild type HsN3, only the Pro-N3-F was detected in the immunoprecipitates of Smad1MH2 (Fig. 4D, lane 4). When COS1 cells were expressing the mutant HsN3 lacking the prosequence, the mutant N3 ( $\Delta$ N3) and  $\Delta$ N3 associated endogenous proteins were detected in the immunoprecipitates of Smad1MH2 (Fig. 4E, lane 4). In addition, four distinct small molecular weight proteins with unknown identity were also recruited into the  $\Delta$ N3/MH2-containing complex (Fig. 4E, lane 2 and lane 4). These four bands were specifically detected only when Smad1MH2 and  $\Delta$ N3 were co-expressed. When Smad1MH2 was replaced with full length Smad1, the  $\Delta$ N3-containing complex was also detected in the immunoprecipitates of Smad1 (Fig. 4F). Thus, a blockage of HsN3 assembly resulted from deleting the prosequence of HsN3 allows the detection of a stable complex between Smad1 and HsN3 assembly intermediates. These data suggest that Smad1 interacts with HsN3 transiently when HsN3 is either in single Pro-HsN3 form, or in Pro-HsN3 assembly intermediates. The lack of mature HsN3 in Smad1 immunoprecipitates does not reflect the inability of Smad1 to bind prosequence-less HsN3, but is likely due to either the trapping/degradation of Smad1 inside of the proteasome, or the rapid dissociation of Smad1 from HsN3. The degradation of Smad1 by proteasome is reported in a separate study [39]. The dissociation of Smad1 from the mature 20S proteasome could be due to the competition of Smad1 binding by a 19S regulator protein or simply due to the inaccessibility of the binding site on HsN3 when two half proteasomes assembly into the mature proteasome.

#### **Two separate domains on Az mediate interaction with Smad1 and HsN3 prior to HsN3 incorporation into the 20S proteasome**

We next examined the interaction between Az and Smad1 in COS1 cells. In the absence of the co-expressed HsN3, Smad1 was co-precipitated with Az (Fig. 5A, top panel, lane 1). The interaction was diminished when cells were co-transfected with the activated BMP type I receptor ALK3Q233D (Fig. 5A, top panel, lane 3). However, the addition of proteasome inhibitor LLnL stabilizes the interaction (Fig. 5A, top panel, lane 2). Thus, Smad1 interacts with Az in mammalian cells and the interaction is also enhanced upon BMP type I receptor activation. In the yeast two-hybrid tests, we also observed the ability of Az to bind HsN3 [39]. Domain mapping analyses of Az reveals two separate domains on Az that are involved in binding to Smad1 and HsN3 (Fig. 5B). In mammalian cells, co-ex-



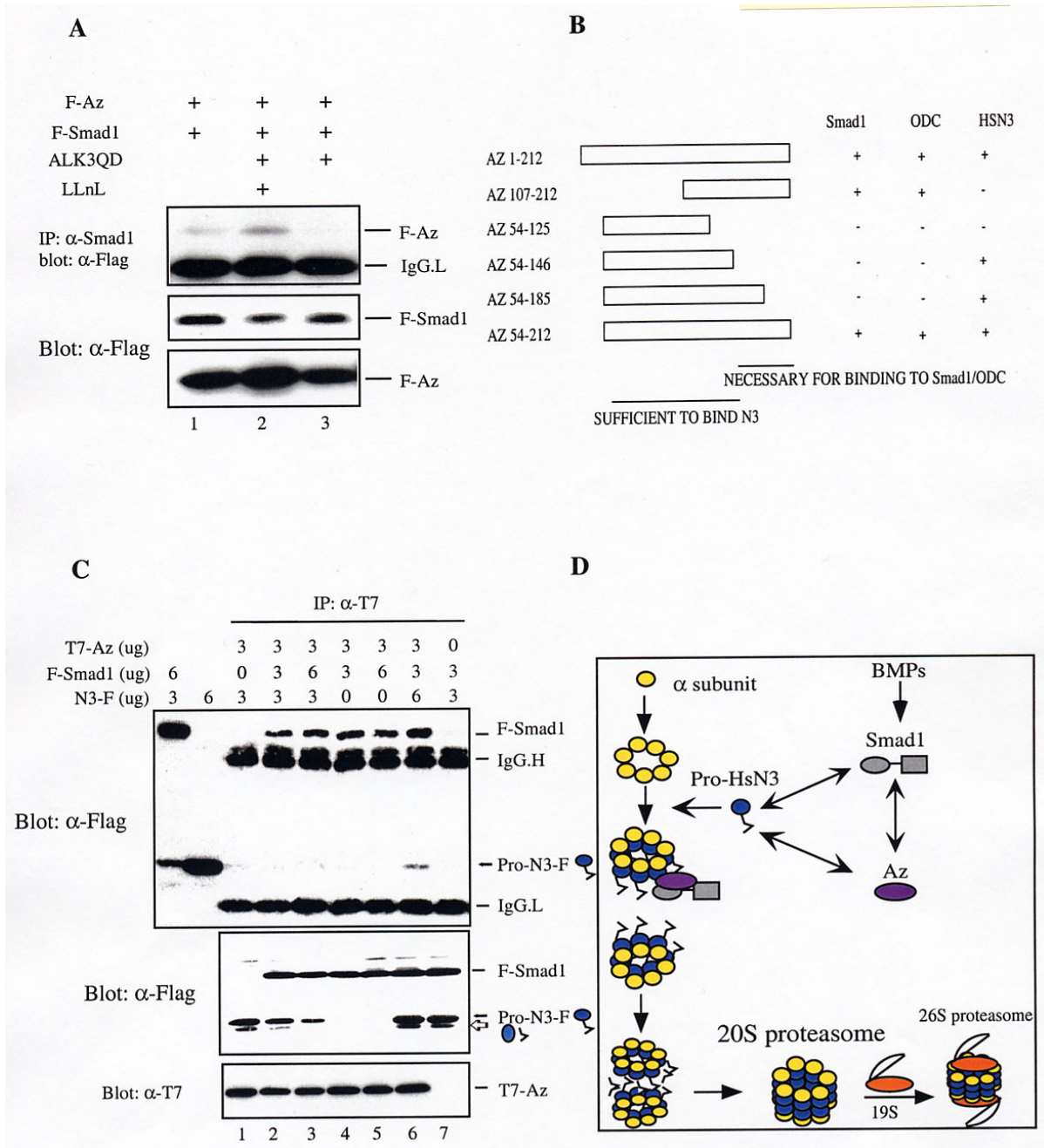


**Figure 5**

**The formation of a ternary complex between Smad I, Az and HsN3.** Az interacts with Smad I and the interaction is enhanced by receptor activation in the presence of lactacystin. COS cells were transfected with the indicated plasmids. F-Smad I was precipitated with anti-Smad I monoclonal antibody and the co-precipitated F-Az was detected by anti-Flag Western blot. "IgG.L." represents the IgG light chain. The total expression of the proteins in the lysates was detected by Western blot as shown in the bottom panels. **B.** Results of domain mapping analyses of Az. Different deletion constructs of Az were made as illustrated and subcloned into yeast expression vector pJG4-5, which were then co-transformed with full length LexA-Smad I and LexA-HsN3 into yeast two-hybrid system. The interaction tests were carried out similarly as shown in Fig. 1. The separate domains important for Az to bind HsN3 and Smad I are indicated. **C.** Az interacts with both Smad I and HsN3 when they are co-expressed at a specific ratio. COS1 cells were co-transfected with the indicated constructs of Smad I, Az and HsN3. The amount of DNA used for the transfection is also indicated. The co-precipitated Smad I and Pro-N3-F are marked. **D.** A cartoon to summarize the observed complex formation between Smad I, HsN3 and Az along the proteasome assembly pathway.

pression of Az with Smad1 and HsN3 leads to the detection of both Smad1 and Pro-N3 in the immunoprecipitates of Az (Fig. 5C, top panel, lane 6). There appears to be a stoichiometric relationship between these three proteins, since the relative levels of these three proteins influence the interaction properties (Fig. 5C). These data suggest that Smad1, Az and HsN3 might form a ternary complex. Since we again only detected the pro-sequence form of HsN3 in Az precipitates, such a ternary complex is likely formed along the assembly pathways of HsN3.

#### **The Activation of the BMP type I receptor induces Smad1-dependent nuclear translocation of both HsN3 and Az**

Smad1 is translocated from the cytoplasm to the nucleus upon its activation by the BMP type I receptors [40]. The physical interaction between Smad1, Az and HsN3 suggests that BMP signaling might regulate the intracellular localization of Az and HsN3. We tested the localization of endogenous HsN3 in COS1 cell line, which was transiently transfected with Smad1, ALK3 and the BMP type II receptor. Cells were either not exposed to BMP2 (Fig. 6A), or treated with BMP2 for 30 mins (Fig. 6B) or 60 mins (Fig. 6C). Cells were stained with a monoclonal anti-HsN3 antibody and FITC-conjugated anti-mouse secondary (Fig. 6A,6B,6C, panels 1) and simultaneously with a polyclonal anti-Smad1 antibody and rhodamine-conjugated anti-rabbit secondary antibody (Fig. 6A,6B,6C, panels 2). The co-localization of Smad1 and HsN3 was detected by overlaying the signals in panels 1 and panels 2 and shown in panels 3. Smad1 and HsN3 were detected in both the cytoplasm and the nucleus in cells that were not exposed to BMP2 (Fig. 6A, panels 1–3). In cells treated with BMP2 for 30 mins, most HsN3 and Smad1 were concentrated in the nucleus (Fig. 6B, panels 1 & 2) and co-localization of Smad1 and HsN3 was detected in the nucleus (Fig. 6B, panel 3). In cells treated with BMP2 for 60 mins, all signals of Smad1 and HsN3 were detected to be co-localized in the nucleus (Fig. 6C, panels 1–3).

We further tested the role of Smad1 in the nuclear translocation of HsN3. HsN3 was detected in speckled pattern throughout the cytoplasm and the nucleus when it was expressed alone in COS1 cells (Fig. 6D, panel 1). Similar localization pattern was detected when HsN3 was co-expressed with Smad1 (Fig. 6D, panel 2) or with ALK3Q233D (Fig. 6D, panel 3). However, when HsN3 was co-expressed with both Smad1 and ALK3Q233D, the majority of HsN3 signals were detected in the nucleus (Fig. 6D, panel 4). Thus, the nuclear translocation of HsN3 is dependent upon both the receptor activation and the presence of Smad1. Similarly, the localization of Az is also dependent upon the co-expression of Smad1 and the activated BMP type I receptor (Fig. 6E, panels 1–4). When Smad1 was replaced by Smad2, Az was found in both the cytoplasm and the nucleus upon the co-expression of

ALK3Q233D (Fig. 6E, panel 4), although cytoplasmic signals of Az were slightly decreased. This could be due to the presence of endogenous Smad1 in COS1 cells.

Thus, the localization of both Az and HsN3 is regulated by the BMP type I receptor in a Smad1-dependent manner. This data confirms the physical interaction between Smad1, HsN3 and Az detected by immunoprecipitation and further suggests that the cytoplasmic Smad1 forms a complex with Az and HsN3 and brings these two proteins into the nucleus upon the activation of BMP type I receptor.

#### **The novel CBP/p300 repressor SNIP1 is recruited to Az upon the activation of BMP type I receptor**

The observed physical interaction between Smad1, HsN3 and Az and the regulation of the complex formation by BMPs suggests a functional role of Az and HsN3 in the signaling function of Smad1. In a separate study, we have shown that Az and HsN3 play targeting roles in the proteasomal degradation of Smad1 upon the activation of BMP type I receptors [39]. The observed proteasomal degradation of Smad1 upon the activation of BMP signaling could simply serve to irreversibly terminate Smad1-mediated signaling pathways of BMPs. However, we observed that Az and HsN3 also interact with several isolated Smad1 interactors. Furthermore, the nuclear co-translocation of Az and HsN3 with Smad1 also suggests potential proteasomal targeting role of Az and HsN3 in the nucleus. Thus, we tested the hypothesis that Az and HsN3 also target Smad1 interacting proteins in the nucleus.

Among the isolated Smad1 interactors shown in Fig. 1, clone 19 encodes a novel nuclear protein named as Smad1 Nuclear Interacting Protein-1 (SNIP-1). Our recent studies suggested that SNIP1 is a novel CBP/p300 repressor [25]. SNIP1, when expressed in COS1 cells, is entirely localized to distinct areas within the nucleus (Fig. 7A). Interestingly, SNIP1 binds to Az and HsN3 in the yeast two-hybrid system, in addition to its ability to bind Smad1 (Fig. 7B). SNIP1 and ODC exhibited similar affinity to Az in the yeast two-hybrid test (Fig. 7B). Domain mapping studies showed that the linker region of Smad1 was sufficient to bind SNIP1 (Fig. 7C). To confirm the interaction between SNIP1 and Az or HsN3 seen in the yeast two-hybrid system, we transfected COS1 cells with each pair of proteins and tested the interactions by immunoprecipitation assays. Upon the co-expression with SNIP1, the pre-assembled form of HsN3 but not Az was co-precipitated with SNIP1 (Fig. 7D, lanes 1 & 2). Since SNIP1 is a nuclear protein, the interaction between SNIP1 and Az may require the nuclear translocation of Az. Based upon the observation that the nuclear translocation of Az is dependent upon Smad1 and BMP type I receptor activation (Fig. 6E), we therefore tested Az interaction with SNIP1 in the pres-

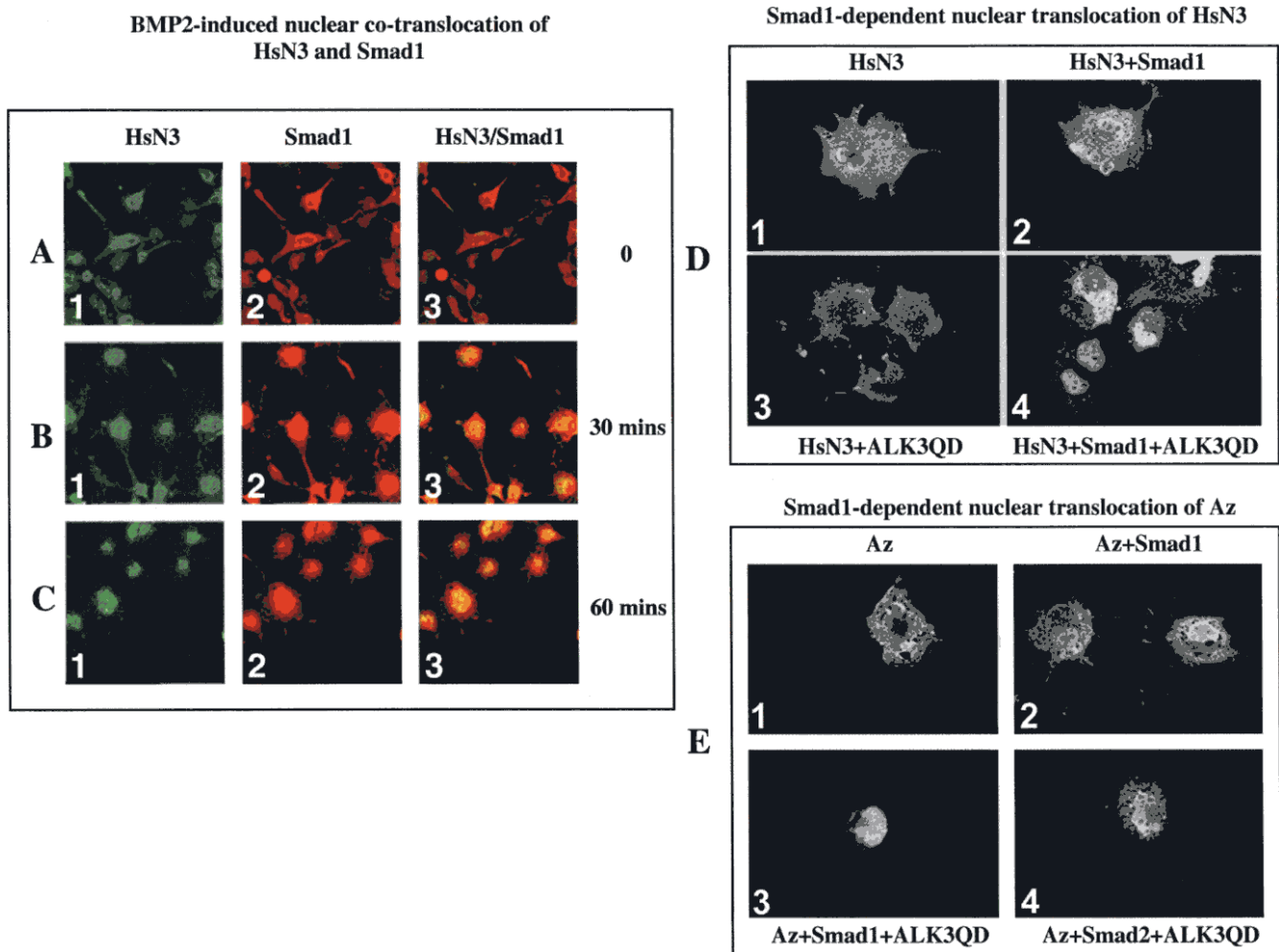


**Figure 6**  
**Smad1-dependent nuclear translocation of Smad1, HsN3 and Az in response to BMP type I receptor activation.** **A-C.** Smad1 and HsN3 are both rapidly translocated from the cytoplasm to the nucleus in response to BMP2. COS cells were transiently transfected with Smad1, ALK3 and BMPRII and were either not treated (A), or treated with BMP2 for 30 mins (B), and 60 mins (C). Smad1 (red) and HsN3 (green) signals at each time point were detected and their co-localization shown by overlaying HsN3 signals in panel "1" with Smad1 signals in panel "2" to yield panel "3". **D.** HsN3 nuclear translocation is dependent upon the coexpression of Smad1 and the activation of the BMP type I receptor. COS cells were transfected with the indicated plasmids. HsN3 was detected by anti-Flag monoclonal antibody and FITC conjugated anti-mouse secondary antibody. **E.** Az is also translocated to the nucleus in response to the activation of BMP type I receptor in a Smad1-dependent fashion. COS cells were transfected with the indicated plasmids and stained with anti-Flag monoclonal antibody and FITC conjugated anti-mouse secondary antibody. To maximize the details of intracellular localization of each protein, each panel only shows the single cell-image that represents the localization patterns in more than 80% transfected cells.

ence of the co-expression of Smad1, Smad4 and ALK3Q233D. In the absence of ALK3Q233D, no F-Az was detected in the precipitates of SNIP1 (Fig. 7E, top panel, lane 2). However, the co-expression of ALK3Q233D allowed the detection of F-Az in SNIP1 immunoprecipitates (Fig. 7E, top panel, lane 3). A weak Smad1 signal but no Smad4 signal was detected in SNIP1 immunoprecipitates.

Thus, in the mammalian overexpression system, the pre-assembled HsN3 exhibits constitutive interaction with SNIP1, whereas Az is only recruited to SNIP1 upon receptor activation. The lack of strong signals of Smad1 or Smad4 in the immunoprecipitates of SNIP1 in the presence of BMP type I receptor activation may be due to the transient nature of the complex, which, as shown below, is targeted to proteasome for degradation.

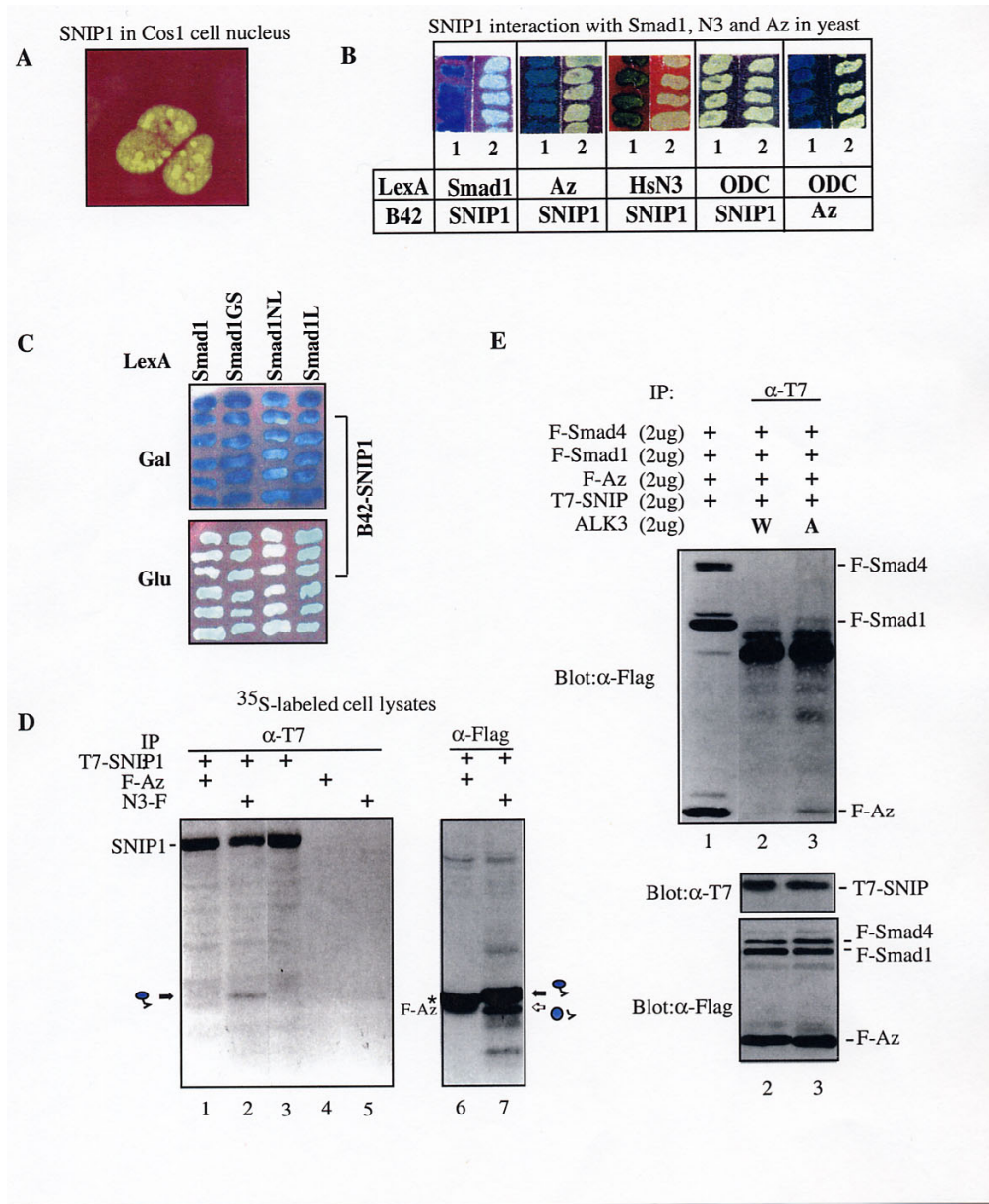


**Figure 7**  
**A novel Smad I Nuclear Interacting Protein (SNIP1) is recruited to interact with Az in a BMP receptor activation-dependent fashion.** **A.** SNIP1 is a nuclear protein. COS1 cells were transfected with T7-tagged SNIP1. Anti-T7 monoclonal antibody and FITC conjugated anti-mouse secondary antibody was used to detect SNIP1. **B.** SNIP1 specifically interacts with Smad1, Az and HsN3 but not with ODC in the yeast two-hybrid system. The panels labeled as "1" and "2" represent yeast transformants on U<sup>14</sup>H<sup>14</sup>W galactose or glucose plates, respectively. B42 fusion proteins were only induced in yeast grown on galactose plates. **C.** Domain mapping of Smad I interaction with SNIP1 in yeast. "Smad1GS" represents the mutant Smad1 (G419S) [40]. Smad1NL contains the MH1 and the linker region; Smad1L contains only the linker region. **D.** SNIP1 interacts with the pro-sequence-containing form of HsN3 but not with Az in COS cells upon coexpression. COS cells were transfected with the indicated plasmids. Cells were metabolically labeled with <sup>35</sup>S-methionine for the last 4 hours before lysates were made for immunoprecipitation. Az is marked by an asterisk in lane 6, while the two forms of HsN3 are marked as in previous Figures. **E.** SNIP1 interacts with Az upon its co-expression with Smad1, Smad4 and the BMP type I receptor activation enhances the interaction. COS cells were transfected with 2  $\mu$ g each of the indicated plasmids. The anti-T7 immunoprecipitates were analyzed by Western blot with monoclonal anti-Flag (top panel). The co-precipitated F-Az is indicated (lane 3). Protein expression was monitored by Western blot analyses of total lysates as shown in bottom panels.

### **BMP type I receptor activation induces SNIP1 degradation that is regulated by Smad1, Smad4 and Az**

To follow the observed reduction of SNIP1 level upon the expression of high level of ALK3Q233D, as mentioned above, we co-expressed SNIP1 together with Smad1, Smad4, Az and high dose (6  $\mu$ g) of either the wild type ALK3 or the constitutive active ALK3Q233D. The protein levels of each protein were analyzed by Western blot (Fig. 8A). A dramatic decrease of SNIP1 level was detected in ALK3Q233D-transfected cells (Fig. 8A, panel 1, lanes 1 & 2). The receptor activation-induced decrease of SNIP1 is partially sensitive to the proteasome-specific inhibitor lactacystin, suggesting the involvement of proteasomal degradation (Fig. 8A, panel 1, lane 3). The incomplete rescue of SNIP1 level by lactacystin suggests the involvement of additional mechanisms other than 26S proteasome in SNIP1 degradation. To systematically demonstrate the role of Smad1, Smad4 and Az in the observed decrease of SNIP1 protein level, we sequentially left out one of these three proteins in the above assay. The ALK3Q233D-induced degradation of SNIP1 was significantly blocked in the absence of Az (Fig. 8A, panel 1, lanes 4 & 5), Smad4 (lanes 6 & 7), or Smad1 (lanes 8 & 9). Thus, the ALK3Q233D-induced degradation of SNIP1 is regulated by the protein levels of Smad1, Smad4, Az and is only induced by high dose of the activated BMP type I receptor. Interestingly, by simply replacing Smad1 with the Smad1 mutant Smad1G419S [40], which is defective in binding to BMP type I receptor for receptor-mediated phosphorylation and the subsequent nuclear translocation, SNIP1 degradation was also inhibited (Fig. 8A, panel 1, lanes 10 & 11), suggesting that the degradation of SNIP1 is dependent upon the type I receptor-mediated phosphorylation of Smad1. The levels of SNIP1 in Fig. 8A top panel are quantified and plotted as Integrated Optical Density (IOD) of SNIP1 (Fig. 8A, right panel).

We noted that the protein levels of Smad1, Smad4 and Az were co-regulated with that of SNIP1. For example, the protein levels of Smad1, Smad4 and Az were all sensitive to lactacystin (Fig. 8A, all panels, compare lane 2 and lane 3). Blocking SNIP1 degradation was accompanied by increased protein levels of Smad1, Smad4 and Az in cells expressing the activated ALK3 (Fig. 8A, lanes 5, 7, 9, 11). The lower levels of Smad1, Smad4, Az and SNIP1 in lane 1 compared with those in lane 10 suggest that the leaky signaling by the overexpressed ALK3, which we have demonstrated recently [39], caused a constitutive reduction of Smad4, Az and SNIP1 level that is dependent upon the activation of Smad1. These data thus suggest that SNIP1 is targeted to proteasome for degradation together with Smad1, Az and Smad4.

The ability of Smad1 in regulating SNIP1 degradation was further demonstrated by increased expression of Smad1 in

COS1 cells that were transfected with a constant amount of Smad4, Az, ALK3Q233D and SNIP1 (Fig. 8B). A dose-dependent effect of Smad1 on receptor-induced degradation of SNIP1 was observed (Fig. 8B, compare lanes 1 & 2 with lanes 5 & 6).

To confirm SNIP1 degradation in non-overexpression systems, we monitored the steady state levels of endogenous SNIP1 in the human keratinocyte HaCaT and mouse myoblast L6. Cells were treated with BMP7 for different periods of time. Western blot analyses using an anti-SNIP1 antibody detected two forms of SNIP1 with slightly different mobility, which are named as SNIP1.A and SNIP1.B (Fig. 8C, top panel). The IOD of each form of SNIP1 as well as the total IOD of both forms are plotted (Fig. 8C, right panel). In HaCaT cells, the protein levels of both forms of SNIP1 were significantly decreased after 3 hrs of BMP7 treatment and were almost diminished by 22 hrs. Interestingly, a different response was observed in L6 cells. The levels of SNIP1 were somewhat increased after 3 hrs and peaked at 3.5 hrs, but then started to decline at 7 hrs and were diminished at 22 hrs.

### **SNIP1 is a nuclear repressor of the BMP-induced transcription responses**

To determine the functional significance of the observed SNIP1 degradation induced by BMPs, we tested the role of SNIP1 in Smad1-regulated gene responses of BMPs. We first tested the effect of SNIP1 on the BMP-induced activation of the Tlx2 promoter, which involves Smad1 [41]. Full length SNIP1 exhibits dose-dependent inhibition of the BMP-induced gene activation, as monitored by the luciferase activities (Fig. 9A). Thus, SNIP1 is an inhibitor of BMP-induced gene response. Since we have previously shown that SNIP1 binds and inhibits CBP/p300 via its N-terminal domain [25], the deletion mutant of SNIP1 lacking the CBP/p300 binding site, SNIP1 (142–369), was tested in the same assay. SNIP1 (142–369) exhibits little inhibitory activity towards the gene response (Fig. 9A, see  $\Delta$ N-SNIP1). This data further suggests that the inhibitory activity of SNIP1 is mediated by its interaction with CBP/p300, similar to what has been reported in the TGF- $\beta$  pathways [25]. We next tested the inhibitory activity of SNIP1 on the transcriptional activity of Smad1, using the GAL4-Smad1 and GAL4-Luc reporter system, as described previously [42,43]. SNIP1 inhibited BMP-induced activation of GAL4-Luc in p19 cells transfected with GAL4-Smad1 (Fig. 9B). The proteasome specific inhibitor lactacystin also inhibited the BMP-induced GAL4-Smad1 transcriptional activity (Fig. 9B), consistent with a role of proteasomal degradation in Smad1-mediated transcription. The effect of lactacystin is specific, since the control reporter gene  $\beta$ -Gal was not inhibited by lactacystin (data not shown). In a separate study, we also demonstrated that proteasomal degradation also plays an essential role

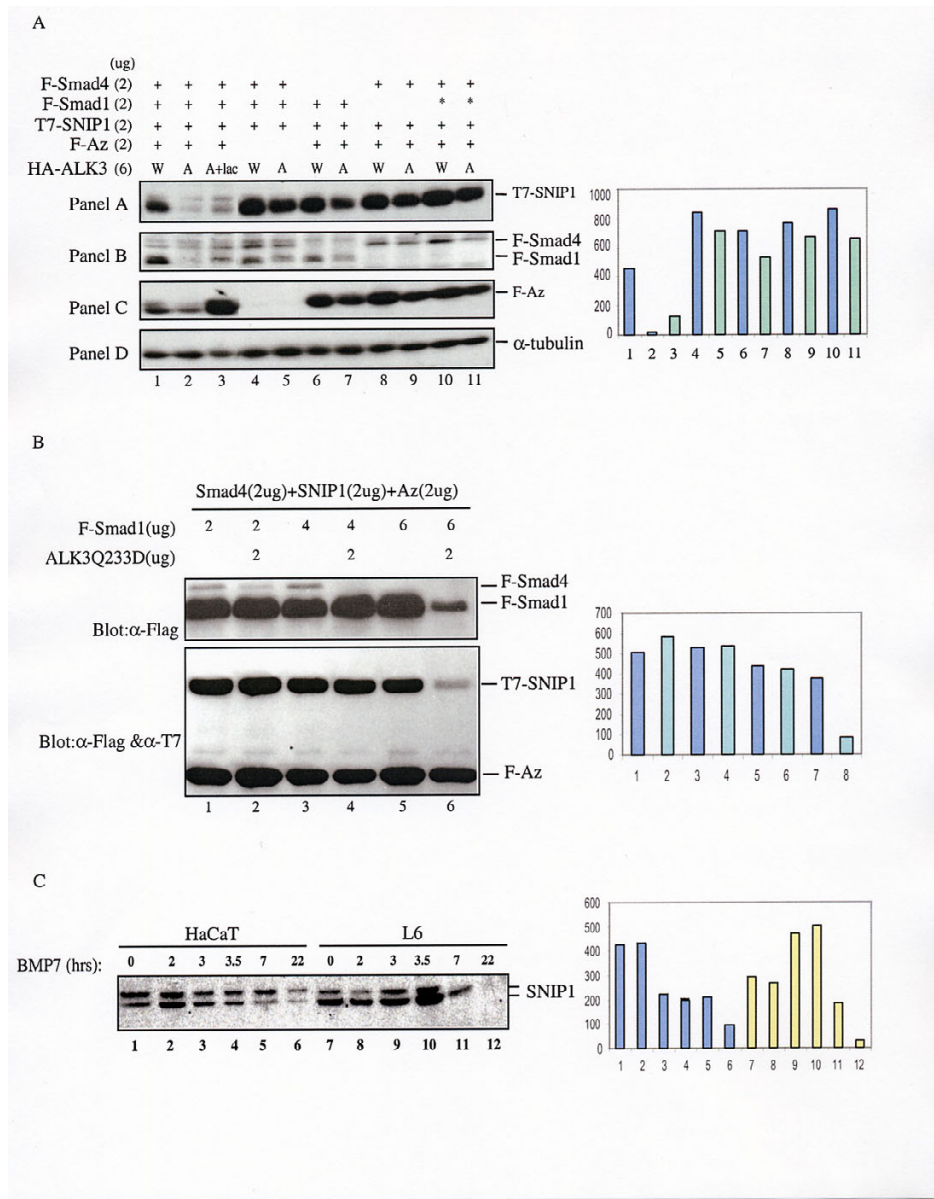


**Figure 8**  
**The activation of BMP type I receptor induces SNIP1 degradation which is co-regulated by Smad1, Smad4 and Az.** **A.** SNIP1 degradation is lactacystin-sensitive and is dependent upon the co-expression of Smad1, Smad4 and Az in COS cell overexpression system. COS cells were transfected with the indicated plasmids. Lactacystin (10  $\mu$ M) was added during the last 10 hrs. The expression of each protein was detected by Western blot. Cell lysates were also blotted with a monoclonal anti- $\alpha$  tubulin, which served as a control for loading (bottom panel). "\*" in lanes 10 and 11 represents the mutant Smad1 (G419S). This construct is T7 tagged, thus did not show on the anti-Flag blot (top panel). Its expression was confirmed by anti-T7 on a separate blot (not shown). The right panel shows the Integrated Optical Density of SNIP1 obtained from quantification of SNIP1 signals using Densitometry. **B.** Increased expression of Smad1 enhances SNIP1 degradation induced by BMP type I receptor activation. COS1 cells were transfected with the indicated amount of DNA constructs of Smad1, Smad4, SNIP1, Az and ALK3Q233D. The protein levels were detected by Western blot. The IOD of SNIP1 is plotted in the right panel. For both panels, equal transfection efficiency was monitored by GFP and equal total protein loading was assured after protein concentration measurement. **C.** The degradation of endogenous SNIP1 is induced in a time-dependent fashion by BMP7 in HaCaT and L6 cells. HaCaT and L6 cells were treated with BMP7 (250 ng/ml) for the indicated time periods and cell lysates were separated on SDS-PAGE then blotted by anti-SNIP1 polyclonal antibody [25]. Two different forms of endogenous SNIP1 are indicated as SNIP1.A and SNIP1.B. The IOD of the combined IOD of these two forms are plotted in the right panel.

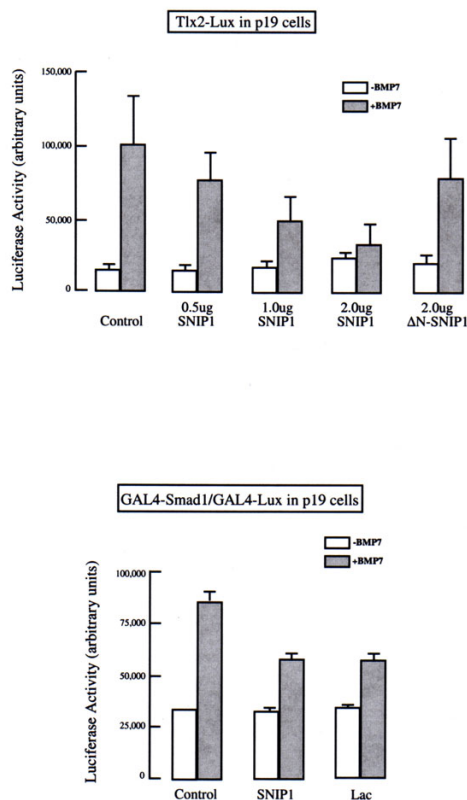


**Figure 9**  
**SNIP1 is a nuclear repressor of Smad1-regulated BMP-induced gene responses.** **A.** Increased expression of SNIP1 inhibits BMP-induced activation of the Tlx-2 reporter gene. P19 cells were transfected with Tlx2-Luc reporter, BMP type I receptor ALK2, the BMP type II receptor BMPRII and different amount of SNIP1, as indicated. ΔN-SNIP: a.a. 142–396, defective in binding to CBP/p300 [25]. BMP7 was added at a final concentration of 250 ng/ml. The arbitrary units of the luciferase activities of each group are presented with error bars. The assays were carried out in triplicate, and similar data were reproduced three times. **B.** Increased expression of SNIP1 or lactacystin treatment both can inhibit BMP-induced transcriptional activity of Smad1-GAL4 fusion protein. P19 cells were transfected with GAL4-Smad1 and GAL4-Luc. Cells were treated with BMP7 (250 ng/ml) 24 hrs before lysates were made for luciferase assays. Lactacystin was added 8 hrs before cells were harvested for the assay.

in BMP induced dendritic formation of rat sympathetic neurons [44].

## Discussion

The bone morphogenetic proteins (BMPs) are multi-functional regulators of early embryogenesis and tissue/organ morphogenesis. Observations made in the past several years suggest that a subset of Smad family proteins play key roles in transmitting the signals of BMPs from the activated receptors at the cell surface to the nucleus to regulate gene expression. Smad1, as one of the three known R-Smads of BMPs, has been extensively studied within the scope of its phosphorylation, interaction with Smad4, nuclear translocation, DNA binding and protein-protein interactions related to its function as a transcriptional regulator. Currently, Smad1 is regarded as a DNA-binding transcriptional modulator that is activated by the BMP type I receptors. Considering the sophisticated mode of regulation characteristic of the TGF- $\beta$ /BMP family ligands, it is expected that that signaling mechanisms of Smads should have a nature of complexity that can accommodate the vast biological functions of these regulators. We took a discovery-driven approach to study the signaling mechanism of Smad1, by systematically searching for proteins that can physically interact with Smad1. Such an approach led to the identification of a set of proteins that can specifically bind to Smad1. This report has focused upon the functional characterization of two proteins that function along the degradation pathways of the 26S proteasome: antizyme (Az) and HsN3.

Az was previously identified as a polyamine-inducible factor that binds and targets the ornithine decarboxylase (ODC) to proteasome for degradation [18,45]. Until now, ODC is the only protein known to be targeted by Az to proteasome, although the existence of additional proteins targeted by Az to proteasome has been suspected [20]. We now find two new Az interactors: Smad1, the key signal transducer of BMPs, as well as SNIP1, the nuclear repressor of CBP/p300. In a separate study, we demonstrated that Smad1 is targeted to proteasome for degradation, a process involving the co-targeting role of Az and HsN3 [39]. Here we showed that SNIP1, after being recruited to Az, is targeted, together with Smad1, to proteasome for degradation. These data indicate that Az has a more general role in targeting different substrates to proteasome for degradation. However, unlike the known ability of Az to bind ODC constitutively, the interaction between SNIP1 and Az is dependent upon the activation of BMP type I receptor and occurs in the presence of Smad1 and Smad4. This suggests the existence of a novel BMP-regulated "conditional" targeting activity of Az that is distinct from the constitutive targeting activity of Az towards ODC.

HsN3 is one of the seven  $\beta$  subunits of the 20S proteasome, which is the catalytic core of the 26S proteasome [22–24]. Besides its role as an indispensable component of the 20S proteasome, HsN3 and the  $\alpha$  subunit HC9 of

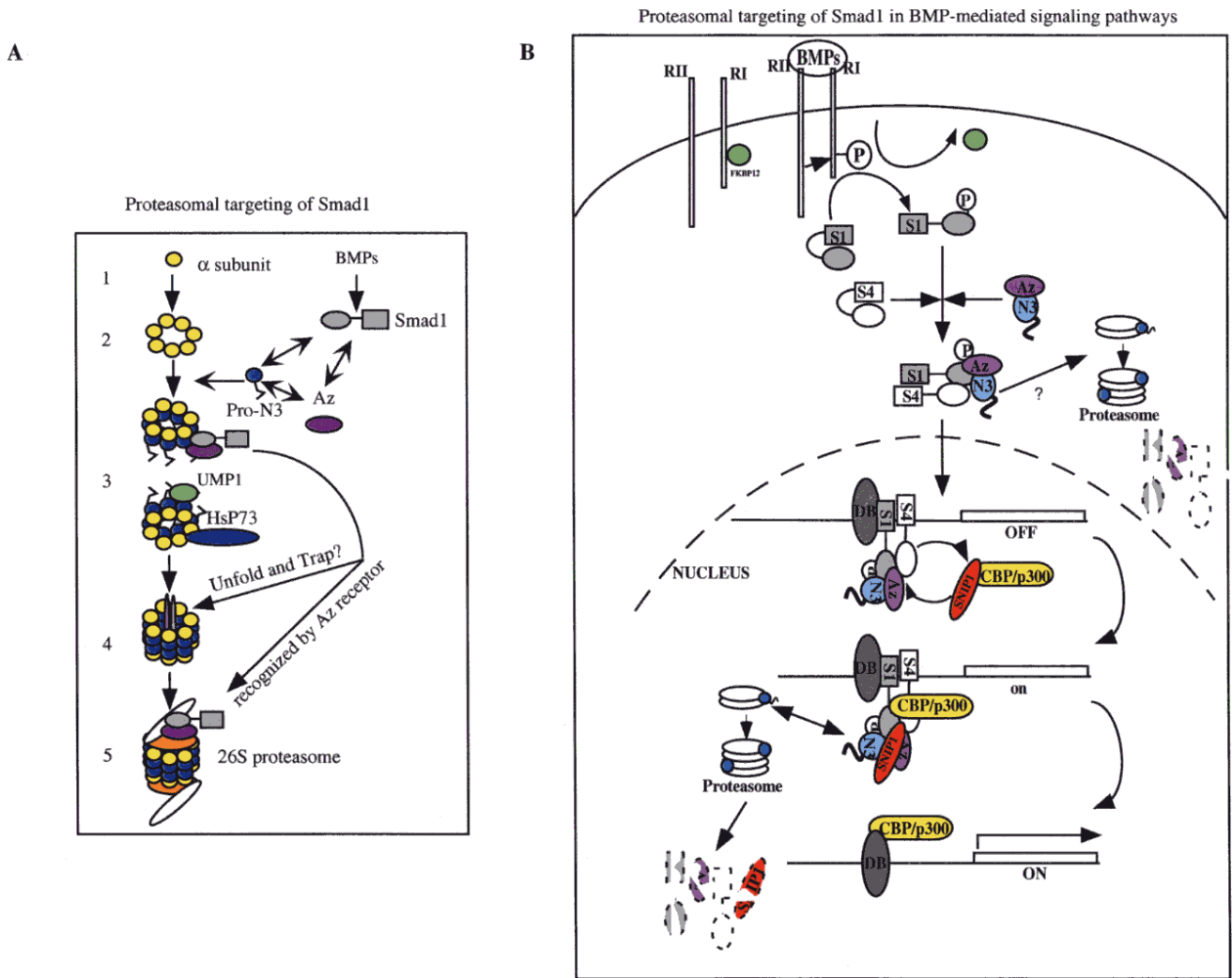


**Figure 10**  
**Mechanisms and functions of proteasomal targeting of Smad1 in signaling pathways of BMPs.**  
**A.** A cartoon to illustrate a novel mechanism for BMP-induced proteasomal targeting of Smad1 induced by BMPs. The activation of BMP type I receptor enhances the interaction between Smad1 and two other proteins Az and HsN3. The newly synthesized HsN3 is in its prosequence-containing form, which forms a ternary complex with Smad1 and Az. The assembly of HsN3 brings Smad1 and Az to assembly intermediates (see step 3). The final maturation of the 20S proteasome may lead to the unfolding and trapping of Smad1 inside the degradation chamber and the ultimate proteasomal degradation of Smad1. Alternatively, Smad1/Az complex may be docked to a receptor of Az on 19S complex for the final delivery of Smad1 to proteasome for degradation. Two other proteins, UMP1 and Hsp73, which are known to be associated with proteasome assembly intermediates, are also shown. Upon the assembly of 20S proteasome, UMP1 is trapped inside of the 20S proteasome for degradation [46]. Hsp73 may play a role in unfolding proteins [35]. **B.** A cartoon to illustrate proteasomal targeting of Smad1 as an integral event along the signaling pathways of BMPs. The activation of the BMP type I receptor is preceded by type II receptor-mediated phosphorylation of the type I receptor and by the dissociation of the cytoplasmic inhibitor FKBP12 from the type I receptor. The activated type I receptor induces Smad1 phosphorylation and the subsequent formation of a complex of Smad1, Smad4, Az and HsN3, which is in its pre-assembled form containing the prosequence. The complex is then translocated into the nucleus, where Smad1 and Smad4 are recruited to specific DNA-binding sites near those of other DNA-binding transcription factors (DBs). In cells where most of the CBP/p300 is bound to SNIP1, the removal of SNIP1 from CBP/p300 may be a critical step for the successful recruitment of CBP/p300 to DBs. One way to remove SNIP1 could be via the recruitment of SNIP1 to Az and HsN3 in the complex containing Smad1 and Smad4. The targeting of Smad1 to proteasome, as illustrated in panel A, could then mediate the co-targeting of SNIP1 to proteasome for degradation. The removal of SNIP1 then allows the subsequent recruitment of CBP/p300 to DBs for transcription. Possible cytoplasmic targeting of Smad1-containing complex via HsN3 assembly pathway is also suggested. See text for details.



the 20S proteasome have been shown to interact with the viral protein Tax. This interaction was suggested to play a role in Tax-induced proteasomal processing of the P105 subunit of NF- $\kappa$ B [32]. Other proteasome integral components, especially those in the 19S regulator of the 26S proteasome, have also been shown to bring proteins to proteasome for degradation [21]. Here we identified a unique role of HsN3 in the Az-involved targeting pathway that is coupled to BMP type I receptor activation. Our data suggests that Smad1 and Az both interact with HsN3 only before HsN3 is fully incorporated into the mature 20S proteasome. We have shown that the reason for Smad1 to only bind to the unprocessed form of HsN3 is not because the prosequence contains a Smad1-binding site. Artificially removing the prosequence of HsN3 in fact allowed Smad1 to stably bind to the prosequence-less HsN3 as well as multiple proteins that are bound to the prosequence-less HsN3, which may represent the assembly intermediates that failed to reach maturation due to the lack of HsN3 prosequence (Fig. 4D,4E,4F). These data collectively point out the transient interaction between Smad1 and HsN3 along the assembly of HsN3 into the 20S proteasome. So far, several proteins have been found to interact with assembly intermediates of the 20S proteasome. A small protein Ump1 associates with the premature proteasome complexes and is shown to be involved in assisting the maturation of 20S proteasome, possibly by interacting with the  $\beta$  rings of half proteasomes [46]. Upon the maturation of the 20S proteasome, Ump1 is trapped inside the proteasome and is degraded by proteasome [46]. The HSP70 like chaperon protein Hsc73 also associates with the 16S proteasome precursor complexes [35,36]. The exact role of Hsc73 in 16S precursor proteasome complex is not known, but has been suggested to assist proteasome maturation [35,36]. Our studies add Smad1, Smad1 interacting proteins such as SNIP1, Smad4, and Az as additional proteins that associate with the assembly intermediates. How does the association of HsN3 contribute to the final degradation or processing of these proteins? Two possible mechanisms are illustrated in Fig. 10A. The first possible mechanism is via "Unfold and Trap". The proteasome assembly intermediates could be a site for the entry of substrates into the degradation chamber via an unfold-trap mechanism that is coupled to the final maturation of the 20S proteasome. The chaperon proteins such as Hsc73 could be involved in unfolding the substrates for them to fit into the degradation chamber and the final maturation of 20S proteasome from the 16S assembly intermediates could trap the substrates, such as Ump1 and Smads, inside the degradation chamber. If so, ubiquitination may not be necessary for the degradation. This could be a common mechanism for ubiquitin-independent degradation pathways. The second possible mechanism is via "docking and delivery". HsN3 may simply bring the Smad/Az containing complex close enough to the 26S proteasome and

then delivers it to the 19S complex via Az interaction with its receptor within 19S regulator.

We have so far identified two functional outcomes of the observed physical interaction between Smad1, HsN3 and Az in the signaling pathways of BMPs. First, in a separate report, we showed that Smad1 itself is targeted to proteasome and is subsequently degraded by the proteasome, an event that is triggered by the activation of BMP type I receptor and involves the targeting role of Az and HsN3 [39]. Proteasomal degradation of Smad1 appears to also play a role in regulating the constitutive level of Smad1 in cell as a way to adjust the cellular responsiveness of BMPs [47]. However, the targeting mechanism and the regulation involved in these two cases of Smad1 degradation by proteasome are likely fundamentally different [39]. The second functional outcome of the physical link between Smad1, HsN3 and Az is the ability of Smad1 to regulate the proteasomal degradation of SNIP1, which is clearly dependent upon high levels of Smad1, Az and a strong activation signal from the type I receptor, as suggested by the observations that the protein levels of Smad1, Az and ALK3Q233D directly influence the degree of SNIP1 degradation. While the detailed mechanisms for such a novel mode of regulation still requires many additional studies, so far we observed several important steps that may contribute to SNIP1 degradation. First, Smad1 binds both HsN3 and Az in the cytoplasm and brings them into the nucleus upon the activation of BMP type I receptor (Fig. 6). Second, SNIP1 is recruited to Az and HsN3, which are likely in a complex with Smad1 and Smad4 (Fig. 7D & 7E). Third, SNIP1 is co-targeted into the proteasome with Smad1, Smad4 and Az via the rapid assembly of HsN3 into the proteasome. This is suggested by the observations that the targeting of SNIP1 is positively regulated by Smad1 level and is dependent upon Smad1, Smad4 and Az (Fig. 8A & 8B). Fourth, Smad4 is a positive regulator of the targeting of SNIP1 to proteasome. The requirement of both Smad1 and Smad4 in the down-regulation of SNIP1 is interesting since this may represent an important molecular mechanism for the co-operative property of these Smads to modulate transcription. The functional significance of SNIP1 degradation is apparent, since SNIP1 is a constitutive interactor and functional repressor of the master transcription co-activator CBP/p300 [25]. In the BMP signaling pathways, SNIP1 is a potent inhibitor of Smad-responsive genes via inhibiting CBP/p300 (Fig. 9A). Thus the down-regulation of SNIP1 likely leads to the liberation of CBP/p300 and directly contributes to the well-known transcriptional modulator functions of Smad1 and Smad4. These ideas are summarized in a cartoon in Fig. 10B. Specifically, the activated Smad1 and Smad4 enter the nucleus, where Smad1 and Smad4 together recruit SNIP1 and CBP/p300. The inhibition of SNIP1 on CBP/p300 is considered to act through its interaction with the

C/H1 domain of CBP/p300, thereby blocking the recruitment of CBP/p300 by other transcription factors including Smad4 [25]. Such an inhibition is counteracted by the ability of Smad4 to compete off SNIP1 from CBP/p300 [25]. So at early phase of Smad activation, although SNIP1 is still bound to Smad1 and Smad4, it is no longer directly bound to CBP/p300, which now can activate transcription. Our data suggested that the Smad1/Smad4 bound SNIP1 can be further targeted to proteasome for degradation. Smad1 and Smad4 are indeed both degraded. However, we propose that such degradation is coupled to the recruitment of the SNIP1-free CBP/p300 to a nearby DNA-binding transcription factor, thus carrying out the commonly observed role of Smads as transcriptional co-modulators. Smads have been shown to mediate transcription via modulating the transcriptional activity of many other DNA-binding proteins. The ability of Smad1 and Smad4 to target SNIP1 for degradation, thereby freeing CBP/p300 for other transcriptional factors is likely an important mechanism for the transcriptional modulator role of these two Smads.

We have observed that several other Smad1 interactors, including some cytoplasmic interactors of Smad1, are also degraded by proteasome (Wang et al., unpublished data). Thus, the location for the targeting of Smad1 may not be limited to only inside of the nucleus, as illustrated in Fig. 10B. Future studies are needed to verify and enrich the details of the illustrated molecular events.

## Conclusions

The subject of proteasomal degradation of Smads and Smad interacting proteins has now become a major focus of interest in the field due to its broad implication in signaling regulation and execution. The work reported here represents our major efforts during the past several years to follow a novel concept of proteasomal degradation in TGF- $\beta$ /BMP signaling based upon the yeast two-hybrid data obtained in 1996. Although there are multiple reports on proteasomal degradation of Smads and Smad interacting proteins, primarily in TGF- $\beta$  signaling pathways [47–54], our observations reported here are entirely based upon our own original observations and show a novel connection of Smads with the proteasome system that no other groups have reported. Our observations provide new revenues for future understanding of the functional mechanisms of Smads, which are likely not limited to transcriptional regulation but are quite extensively linked to the regulation of proteasomal degradation of multiple cytoplasmic and nuclear proteins.

## Materials and Methods

### Construction of expression plasmids

For the yeast two-hybrid screen, full-length Smad1 was subcloned into BamH1/Not1 sites of PEG202 by a PCR

method, resulting in the inframe fusion between the LexA DNA binding domain (1–202) and Smad1. The Smad1 (G419S) mutant was a kind gift from J. Wrana [40]. The subcloning of Smad1 (G419S), Smad1NL (1–271), Smad1L (147–271) into pEG202 were all carried out similarly by the PCR approach. The mammalian expression constructs of Smad1 and its deletion mutant Smad1C (271–465) were made by subcloning Smad1 into two modified pCMV6 vectors, which have either the Flag epitope (F-pCMV6) or the T7 epitope (T7-pCMV6) placed upstream of an array of new multiple cloning sites. T7- $\Delta$ N3 pCMV6 was made by PCR amplification of HsN3 (a.a. 45–263) followed by subcloning the PCR products into the EcoR1/Xho1 sites of the modified T7-pCMV6 vector. N3-F pCMV6 was made by PCR amplification of HsN3 (1–263) followed by subcloning the PCR products into the EcoR1/EcoRV sites of pFlag-CMV5C vector (Kodak). The fidelity of the PCR products was determined by DNA sequencing. The constitutively active mutant BMP type I receptor (ALK3Q233D) is a gift from J. Massagué; Tlx-2 reporter is from J. Wrana; full length rat Az is from P. Coffino.

### Yeast two-hybrid screen and tests

A modified yeast two-hybrid system developed by Brent and colleagues [26,27] was used to isolate Smad1 interactors. Briefly, yeast strain EGY48 (leu2, his3, trp1, ura3), which has an integrated Leu2 reporter, was first transformed with a LexAop-LacZ reporter. The selected transformants were transformed again with the bait construct Smad1pEG202. The selected bait transformants were transformed with a human fetal brain cDNA library (a gift from Roger Brent). About one million original transformants were obtained. From the pooled stock of the transformants, ten million cells were screened on U·H·W·L galactose plates containing X-Gal (5-bromo-4-chloro-3-indolyl- $\beta$ -D-galactosidase). Only those that form blue colonies were picked as candidate positives. The cDNAs from the candidate positives were purified, re-tested for Smad1 interaction in yeast, and then sequenced. For testing protein-protein interaction using the yeast two-hybrid system, the same yeast strain was first transformed with the LexA-fusion construct, selected on U·H· plates, then re-transformed with B42-fusion constructs, and selected on U·H·W· plates. The transformants were first streaked onto a master plate, then replicated onto two testing plates: U·H·W· glucose plate with X-Gal and U·H·W· galactose/raffinose plate with X-Gal. For presentation, yeast transformants were also directly streaked onto U·H·W· galactose/raffinose plate with X-Gal, after confirming lack of the auto-activation on glucose plates.

### **Transient transfection, <sup>35</sup>S-metabolic labeling, immunoprecipitation and western blot**

Equal amount of total plasmids were used to transiently transfect COS-1 using the DEAE dextran method [40]. A GFP construct was used to monitor the transfection efficiency. 293 cells were transfected by the standard CaPO<sub>4</sub> procedure [55] and cells were harvested 24 hrs after transfection. For metabolic labeling, cells were incubated with 250 μCi <sup>35</sup>S-methionine per plate for 4 hrs, two days after transfection. To make lysates, transfected cells were washed with cold HBSS, scraped, lysed on ice in 300 μl lysis buffer (20 mM Tris, PH 7.4, 150 mM NaCl, and 0.5% Triton X-100, 1mM EDTA) containing protease inhibitors. Protein expression level was determined by Western blot analyses of 20 μl lysates before any immunoprecipitation assays. For immunoprecipitation, 150 μl cell lysates were pre-cleaned by protein A sepharose beads (Pharmacia), incubated with 3 μl of anti-T7 (1 mg/ml) or anti-Flag (3 mg/ml) (M2 monoclonal, IBI, Eastman Kodak) on ice overnight. Protein A (for anti-T7) and protein G (for anti-Flag) sepharose beads were used to absorb the antibodies. After washing, beads were treated with protein sample buffer to elute immunoprecipitates. Eluted proteins were separated on SDS-PAGE. The detection of the co-precipitated proteins was carried out either by autoradiography, if proteins were metabolically labeled or by Western blot using the ECL kit. When proteasome inhibitors were applied, the inhibitors LLnL (50 mM in DMSO) or lactacystin (10 mM in H<sub>2</sub>O) were added directly to the cell medium at 1:1000 dilutions. Lactacystin was purchased from E. J. Corey laboratory at Harvard University. LLnL was purchased from Sigma.

### **Immunocytochemistry and confocal microscopy**

Immunocytochemistry was carried out as described previously [40]. Briefly, COS cells were grown to 50% confluency on gelatin-coated glass cover slips. Cells were transiently transfected with the indicated plasmids (total 10 μg) using the DEAE dextran method. About 48 hrs after transfection, cells were fixed in 4% paraformaldehyde for 10 min, and then permeabilized with methanol for 2 mins. Cells were blocked in 10% goat serum/PBS for 1 hr at room temperature, before the sequential incubation with the primary and secondary antibodies. The monoclonal anti-HsN3 (MCP444) is a gift from K. B. Hendil. The polyclonal anti-Smad1 antibody is a gift from A. Roberts. The secondary antibodies were either FITC-conjugated, or Rodamine-conjugated goat anti-mouse IgG (Jackson ImmunoResearch, Westgrove PA).

Confocal Microscopy was carried out on a Leica TCS 4D Confocal Laser Scanning Microscope at the Schepens Eye Research Institute (Boston MA).

### **Luciferase assays**

P19 cells were seeded in 100 mm dish and cultured for 24 hrs before they were transfected with luciferase reporter constructs using Fugene Kit (Roche). Each group of transfected cells was re-seeded into eight separate wells in a 24-well plate 18 hrs after transfection. Eighteen hrs after re-seeding, cells were washed twice with 1 ml serum-free media and left in 200 μl media. Four out of eight dishes of each group were exposed to BMP7 (25 ng/ml BMP7), which was directly added into the media for 24 hrs. Culture media was then removed and 100 μl of Reporter Lysis Buffer (Promega 5X stock, diluted with H<sub>2</sub>O) was added to the cells, which were then frozen at -80°C for 3 hrs. The plates were thawed and 70 μl of supernatant was transferred to luciferase plates, mixed with 70 μl of luciferase reagent (Promega). The luciferase activity was detected on Wallac Victor 1420 plate reader. To normalize data, cells were also transfected with β-Gal reporter and the β-galactosidase activities measured using the Galacto-star kit (Tropix, BM300S).

### **Authors' contributions**

Y. L. carried out most of the immunoprecipitation experiments to confirm the protein-protein interactions presented in the paper. J. M. carried out most of the yeast two-hybrid system studies. C. G. carried out the domain mapping studies for Az interaction with Smad1 and HsN3. J. F. carried out the studies to determine the endogenous level change of SNIP1 in response to BMPs; X. M. and B.-Y. L. carried out all preparations of the constructs and many technical supports. R.L. provided the bait construct for the yeast two-hybrid screen study of Smad1 and worked with C.H. and R. H. K. to screen and clone the full length clone of SNIP1. W.G. and V. P. carried out functional studies of SNIP1 in BMP-responsive cells. T. W. conceived the study, participated in its design and coordination and the preparation of the Figures and texts of the paper.

All authors read and approved the final manuscript.

### **Acknowledgments**

We thank P. Andriess and S. Guedes for technical art work; J. Farley, P. Danielson for technical assistance, J. Massagué for ALK3Q233D and BMPRII constructs; C. Heldin for ALK3 construct; J. Wrana for constructs of Smad1 (G419S), Smad2, Tlx-2-Lux, GAL4-Smad1 and GAL4-Lux constructs; R. Derynck for Smad3 construct; A. Roberts for Smad1 construct and polyclonal anti-Smad1; P. Coffino for cDNAs of Az and ODC; E.J. Corey for lactacystin; K. Sampath at the Creative BioMolecule Inc. for BMP7; The Genetic Institute Inc. for BMP2; K.B. Hendil for anti-HsN3; and R. Brent and A. Zervos for the "Protein Trap" system and the brain cDNA library.

### **References**

1. Harland RM: **The transforming growth factor beta family and induction of the vertebrate mesoderm: bone morphogenetic proteins are ventral inducers [comment].** *Proc Natl Acad Sci U S A* 1994, **91**:10243-10246

2. Hogan BL: **Bone morphogenetic proteins: multifunctional regulators of vertebrate development.** *Genes Dev* 1996, **10**:1580-1594
3. Kingsley DM: **The TGF-beta superfamily: new members, new receptors, and new genetic tests of function in different organisms.** *Genes Dev* 1994, **8**:133-146
4. Reddi AH: **Regulation of cartilage and bone differentiation by bone morphogenetic proteins.** *Curr Opin Cell Biol* 1992, **4**:850-855
5. Kawabata M, Imamura T, Miyazono K: **Signal transduction by bone morphogenetic proteins.** *Cytokine Growth Factor Rev* 1998, **9**:49-61
6. Massague J: **TGF-beta signal transduction.** *Annu Rev Biochem* 1998, **67**:753-791
7. Wrana JL: **Regulation of Smad activity.** *Cell* 2000, **100**:189-192
8. Zhang Y, Derynck R: **Regulation of Smad signalling by protein associations and signalling crosstalk.** *Trends Cell Biol* 1999, **9**:274-279
9. Kawabata M, Inoue H, Hanyu A, Imamura T, Miyazono K: **Smad proteins exist as monomers in vivo and undergo homo- and hetero-oligomerization upon activation by serine/threonine kinase receptors.** *EMBO J* 1998, **17**:4056-4065
10. Massague J, Chen YG: **Controlling TGF-beta signaling.** *Genes Dev* 2000, **14**:627-644
11. Attisano L, Wrana JL: **Smads as transcriptional co-modulators.** *Curr Opin Cell Biol* 2000, **12**:235-243
12. Kim J, Johnson K, Chen HJ, Carroll S, Laughon A: **Drosophila Mad binds to DNA and directly mediates activation of vestigial by Decapentaplegic.** *Nature* 1997, **388**:304-308
13. de Caestecker MP, Yahata T, Wang D, Parks WT, Huang S, Hill CS, et al: **The Smad4 activation domain (SAD) is a proline-rich, p300-dependent transcriptional activation domain.** *J Biol Chem* 2000, **275**:2115-2122
14. Verschuere K, Remacle JE, Collart C, Kraft H, Baker BS, Tylzanowski P, et al: **SIP1, a novel zinc finger/homeodomain repressor, interacts with Smad proteins and binds to 5'-CACCT sequences in candidate target genes.** *J Biol Chem* 1999, **274**:20489-20498
15. Shi X, Yang X, Chen D, Chang Z, Cao X: **Smad1 interacts with homeobox DNA-binding proteins in bone morphogenetic protein signaling.** *J Biol Chem* 1999, **274**:13711-13717
16. Nakashima K, Yanagisawa M, Arakawa H, Kimura N, Hisatsune T, Kawabata M, et al: **Synergistic signaling in fetal brain by STAT3-Smad1 complex bridged by p300 [see comments].** *Science* 1999, **284**:479-482
17. Coux O, Tanaka K, Goldberg AL: **Structure and functions of the 20S and 26S proteasomes.** *Annu Rev Biochem* 1996, **65**:801-847
18. Hayashi S, Murakami Y, Matsufuji S: **Ornithine decarboxylase antizyme: a novel type of regulatory protein.** *Trends Biochem Sci* 1996, **21**:27-30
19. Chen P, Hochstrasser M: **Autocatalytic subunit processing couples active site formation in the 20S proteasome to completion of assembly.** *Cell* 1996, **86**:961-972
20. Pickart CM: **Targeting of substrates to the 26S proteasome.** *FASEB J* 1997, **11**:1055-1066
21. Tanaka K, Chiba T: **The proteasome: a protein-destroying machine.** *Genes Cells* 1998, **3**:499-510
22. Cruz M, Nandi D, Hendil KB, Monaco JJ: **Cloning and characterization of mouse Lmp3 cDNA, encoding a proteasome beta subunit.** *Gene* 1997, **190**:251-256
23. Kopp F, Kristensen P, Hendil KB, Johnsen A, Sobek A, Dahlmann B: **The human proteasome subunit HsN3 is located in the inner rings of the complex dimer.** *J Mol Biol* 1995, **248**:264-272
24. Thomson S, Rivett AJ: **Processing of N3, a mammalian proteasome beta-type subunit.** *Biochem J* 1996, **315**(Pt 3):733-738
25. Kim RH, Wang D, Tsang M, Martin J, Huff C, de Caestecker MP, et al: **A novel smad nuclear interacting protein, SNIP1, suppresses p300-dependent TGF-beta signal transduction.** *Genes Dev* 2000, **14**:1605-1616
26. Brent R, Finley RL Jr: **Understanding gene and allele function with two-hybrid methods.** *Annu Rev Genet* 1997, **31**:663-704
27. Zervos AS, Gyuris J, Brent R: **Mx1, a protein that specifically interacts with Max to bind Myc-Max recognition sites [published erratum appears in Cell 1994 Oct 21;79(2):following 388].** *Cell* 1993, **72**:223-232
28. Ray R, Miller DM: **Cloning and characterization of a human c-myc promoter-binding protein.** *Mol Cell Biol* 1991, **11**:2154-2161
29. Gross B, Gaestel M, Bohm H, Bielka H: **cDNA sequence coding for a translationally controlled human tumor protein.** *Nucleic Acids Res* 1989, **17**:8367
30. Prosperi MT, Ferbus D, Karczynski I, Goubin G: **A human cDNA corresponding to a gene overexpressed during cell proliferation encodes a product sharing homology with amoebic and bacterial proteins.** *J Biol Chem* 1993, **268**:11050-11056
31. Parks WT, Frank DB, Huff C, Renfrew HC, Martin J, Meng X, et al: **Sorting Nexin 6, a Novel SNX, Interacts with the Transforming Growth Factor-beta Family of Receptor Serine-Threonine Kinases.** *J Biol Chem* 2001, **276**:19332-19339
32. Rousset R, Desbois C, Bantignies F, Jalinot P: **Effects on NF-kappa B1/p105 processing of the interaction between the HTLV-I transactivator Tax and the proteasome.** *Nature* 1996, **381**:328-331
33. Frentzel S, Pesold-Hurt B, Seelig A, Kloetzel PM: **20 S proteasomes are assembled via distinct precursor complexes. Processing of LMP2 and LMP7 proproteins takes place in 13-16 S pre-proteasome complexes.** *J Mol Biol* 1994, **236**:975-981
34. Nandi D, Woodward E, Ginsburg DB, Monaco JJ: **Intermediates in the formation of mouse 20S proteasomes: implications for the assembly of precursor beta subunits.** *EMBO J* 1997, **16**:5363-5375
35. Schmidt M, Schmidtke G, Kloetzel PM: **Structure and structure formation of the 20S proteasome.** *Mol Biol Rep* 1997, **24**:103-112
36. Schmidtke G, Schmidt M, Kloetzel PM: **Maturation of mammalian 20 S proteasome: purification and characterization of 13 S and 16 S proteasome precursor complexes.** *J Mol Biol* 1997, **268**:95-106
37. Kruger E, Kloetzel P, Enekel C: **20S proteasome biogenesis.** *Biochimie* 2001, **83**:289-293
38. Groll M, Ditzel L, Lowe J, Stock D, Bochtler M, Bartunik HD, et al: **Structure of 20S proteasome from yeast at 2.4 A resolution [see comments].** *Nature* 1997, **386**:463-471
39. Gruendler C, Lin Y, Farley J, Wang T: **Proteasomal degradation of Smad1 induced by bone morphogenetic proteins.** *J Biol Chem* 2001, **276**:46533-46543
40. Hoodless PA, Haerry T, Abdollah S, Stapleton M, O'Connor MB, Attisano L, et al: **MADRI, a MAD-related protein that functions in BMP2 signaling pathways.** *Cell* 1996, **85**:489-500
41. Macias-Silva M, Hoodless PA, Tang SJ, Buchwald M, Wrana JL: **Specific activation of Smad1 signaling pathways by the BMP7 type I receptor, ALK2.** *J Biol Chem* 1998, **273**:25628-25636
42. Liu F, Hata A, Baker JC, Doody J, Carcamo J, Harland RM, et al: **A human Mad protein acting as a BMP-regulated transcriptional activator [see comments].** *Nature* 1996, **381**:620-623
43. Hayashi H, Abdollah S, Qiu Y, Cai J, Xu YY, Grinnell BW, et al: **The MAD-related protein Smad7 associates with the TGFbeta receptor and functions as an antagonist of TGFbeta signaling.** *Cell* 1997, **89**:1165-1173
44. Guo X, Lin Y, Horbinski C, Drahushuk KM, Kim I-J, Kaplan PL, Lein P, Wang T, Higgins D: *J Neurobiology* 2001, **48**:120-130
45. Matsufuji S, Inazawa J, Hayashi T, Miyazaki Y, Ichiba T, Furusaka A, et al: **Assignment of the human antizyme gene (OAZ) to chromosome 19p13.3 by fluorescence in situ hybridization.** *Genomics* 1996, **38**:102-104
46. Ramos PC, Hockendorff J, Johnson ES, Varshavsky A, Dohmen RJ: **Ump1p is required for proper maturation of the 20S proteasome and becomes its substrate upon completion of the assembly.** *Cell* 1998, **92**:489-499
47. Zhu H, Kavsak P, Abdollah S, Wrana JL, Thomsen GH: **A SMAD ubiquitin ligase targets the BMP pathway and affects embryonic pattern formation.** *Nature* 1999, **400**:687-693
48. Stroschein SL, Wang W, Zhou S, Zhou Q, Luo K: **Negative feedback regulation of TGF-beta signaling by the SnoN oncoprotein [see comments].** *Science* 1999, **286**:771-774
49. Sun Y, Liu X, Ng-Eaton E, Lodish HF, Weinberg RA: **SnoN and Ski protooncoproteins are rapidly degraded in response to transforming growth factor beta signaling.** *Proc Natl Acad Sci U S A* 1999, **96**:12442-12447
50. Lo RS, Massague J: **Ubiquitin-dependent degradation of TGF-beta-activated Smad2.** *Nat Cell Biol* 1999, **1**:472-478
51. Ebisawa T, Fukuchi M, Murakami G, Chiba T, Tanaka K, Imamura T, et al: **Smurf1 interacts with transforming growth factor-beta type I receptor through Smad7 and induces receptor degradation.** *J Biol Chem* 2001, **276**:12477-12480

52. Kavsak P, Rasmussen RK, Causing CG, Bonni S, Zhu H, Thomsen GH, et al: **Smad7 binds to Smurf2 to form an E3 ubiquitin ligase that targets the TGF beta receptor for degradation.** *Mol Cell* 2000, **6**:1365-1375
53. Zhang Y, Chang C, Gehling DJ, Hemmati-Brivanlou A, Derynck R: **Regulation of Smad degradation and activity by Smurf2, an E3 ubiquitin ligase.** *Proc Natl Acad Sci U S A* 2001, **98**:974-979
54. Lin X, Liang M, Feng XH: **Smurf2 is a ubiquitin E3 ligase mediating proteasome-dependent degradation of Smad2 in transforming growth factor-beta signaling.** *J Biol Chem* 2000, **275**:36818-36822
55. Ausubel FM: *In Current Protocols in Molecular Biology.* (Edited by: Janssen K) New York: John Wiley & Sons; 1994, 1-20

Publish with **BioMed** Central and every scientist can read your work free of charge

*"BioMedcentral will be the most significant development for disseminating the results of biomedical research in our lifetime."*

Paul Nurse, Director-General, Imperial Cancer Research Fund

Publish with **BMC** and your research papers will be:

- available free of charge to the entire biomedical community
- peer reviewed and published immediately upon acceptance
- cited in PubMed and archived on PubMed Central
- yours - you keep the copyright



Submit your manuscript here:

<http://www.biomedcentral.com/manuscript/>

[editorial@biomedcentral.com](mailto:editorial@biomedcentral.com)